ARTICLE

Materials interacting with inorganic selenium from perspective of electrochemical sensing

Received 00th January 20xx,
Accepted 00th January 20xx

DOI: 10.1039/x0xx00000x

Jaroslav Filip,*[a] Štěpán Vinter, [a] Erika Čechová [a] and Jitka Sotolářová [a]

Inorganic selenium, the most common form of harmful selenium in the environment, can be determined using electrochemical sensors, which are compact, fast, reliable and easy-to-operate devices. Despite the progress in this area, there is still significant room for developing high-performance selenium electrochemical sensors. To achieve this, one should take into account i) the electrochemical process that selenium undergo on the electrode; ii) valent state of selenium species in the sample and iii) modification of the sensor surface by material with high affinity to selenium. The goal of this review is to provide the knowledge base on these issues. After the Introduction section, mechanisms and principles of the electrochemical reduction of selenium are introduced, followed by a section introducing the modification of electrodes with materials interacting with selenium and the section dedicated to speciation methods, including reduction of non-detectable Se(VI) to detectable Se(IV). In the following chapters, main types of materials (metallic, polymers, hybrid (nano)materials…) interacting with inorganic selenium (mostly absorbents) are reviewed to show the diversity of properties that may be cast to sensors if the materials would be used for modification of electrodes. These features for main material categories are outlined in the conclusion section, where it is stated that the engineered polymers may be the most promising modifiers.

1 Introduction

Selenium (Se) is a non-metal element which rarely occurs in the earth's crust, with an average concentration from 0.05 to 0.09 mg/kg, as pure ore compounds or in its elemental state [1]. Selenium is classified as a precedence pollutant, and it is the constituent of various sulphide minerals and metallic ores [2]. It is released from natural (weathering Se-containing rocks and volcanic eruptions) and anthropogenic sources (combustion of coal) [3,4]. Furthermore, the applications of selenium in the different industrial processes such as electronics, paint industry, metallurgy, and agriculture were reported [3,5]. The fate of Se in the environment is mainly determined by its oxidation state, and it is dependent on pH, pE and biological activity [6]. The Se is stable in four valence states, that is, selenide (Se^{2-}), elemental selenium (Se^0), selenite (Se^{4+}, Se(IV), SeO_3^{2-}), and selenate (Se^{6+}, Se(VI), SeO_4^{2-}), which is the most bioavailable and soluble compound in the oxidizing environment [7]. Thus, the most abundant compounds are selenites and selenates, which prevail as diselenite ion Se_2O_5 and selenate anion SeO_4^{2-} in the pH range between 3.5 and 9 [6]. Under highly reducing conditions elemental selenium (Se^0) is predicted to form which can then be reduced to selenide (Se(-II)). Selenides form metal and organoselenides and can often be found in sediments and rocks as mineral phases. In general, inorganic species of Se are more toxic than the organic forms, with Se(IV) being more toxic than Se(VI).

Selenium in the environment

The natural selenium sources in surface **waters** are atmospheric wet, dry deposition, surface runoff, while effluents of sewage treatment plants, fly ash settling ponds, hazardous waste sites and mining activities [1] are typical anthropogenic sources. Selenium levels in wastewaters from these sites can be as high as 2100 mg kg^{-1} [8], while mine waste can contain up to 111 mg kg^{-1} selenium or rich selenium

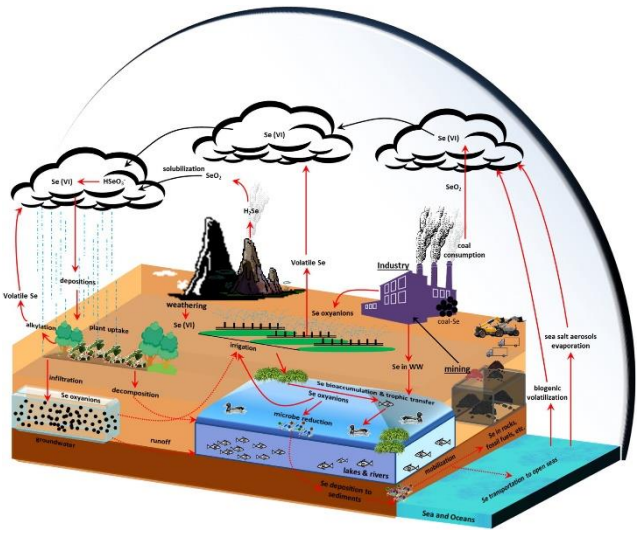

Figure 1: Global geobiochemical cyclus of selenium. Reprinted with permission from Tan et al., 2016 [4], copyright Elsevier, 2016.

[a] Department of Environmental Protection Engineering, Faculty of Technology, Tomas Bata

Electronic Supplementary Information (ESI) available: [details of any supplementary information available should be included here]. See DOI: 10.1039/x0xx00000x

Table 1: Selected studies on determination of inorganic selenium in waters including sensing properties and theoretical maximum sorption capacity of the material employed in sensors.

Analyte	Type of electrode/adsorbent	LOD	Linear range	Absorption capacity	Analytical technique	EC limit	Ref.
Se(IV)	Immobilization of N,N'-di(3-carboxysalicylidene)-3,4-diamino-5-hydroxypyrazole onto the mesoporous silica monolith	1.14 µg L^{-1}	NA	112.12 mg g^{-1}	ICP-AES	✓	20
Se(IV)	Graphene oxide-TiO_2 nanocomposite pH 0.5-10	0.04 µg L^{-1}	0.1-12 ng/mL	3.77 mg g^{-1}	GFAAS	✓	21
Se(IV)	Al_2O_3 nanoparticles functionalized with Aliquat-336 pH 7.0	1.4 ng L^{-1}	5-120 µg/L	35.3 mg g^{-1}	ICP-OES	✓	22
Se(IV), Se(VI)	NA	2.4 and 18.6 ng mL^{-1}	DL-250 and DL-750	NA	HPLC-HG-AAS	✓	23
Se(IV), Se(VI)	Nano sized TiO_2 colloid	24 ng L^{-1} and 48 ng L^{-1}	0-1000 µg/L	0.4 and 27.10 mg g^{-1}	HG-AFS	✓	24
Se(VI)	Fe-impregnated biochar from food waste	3.2 µg L^{-1}	NA	11.7 mg g^{-1}	ICP-OES	✓	25
$SeCN^-$, Se(IV), Se(VI)	NA	0.35; 0.56 and 1.67 µg L^{-1}	NA	NA	GC-MS	✓	26
(SeO_3^{2-}), Se(IV)	SiO_2 nanoparticles (NPs) grafted with 3-(2-aminoethylamino) propyltrimethoxysilane in an acidic medium in the presence of Se(IV) (template ion). Thin surface-imprinted layers of selenite were formed on SiO_2 NPs.	11.33 µg L^{-1}	15 to 100 µg L^{-1}	469.48 µg g^{-1}	UV-1800 spectrophoto meter	x	27
Se (IV)	Pencil graphite electrode modified with a film of acetophenone, polypyrrole and copper nanoparticles	16.58 mM	50 to 110 nM	NA	cyclic and square wave voltammetry	NA	28
Se(IV), Se(VI)	Gold, modified boron doped diamond electrodes	20 and 50 µg L^{-1}	2 to 10 mg/L	NA	cyclic voltammetry	x	29
Se (IV)	Platinum and gold electrodes - milimetre sized gold electrode microband electrode array	1.2 µM 25 nM	5-15 µm 0.1-10 µM	NA	square wave anodic stripping voltammetry	x	30
Se (IV)	Au electrode	0.04 µg L^{-1}	NA	NA	stripping voltammetry	✓	31
Se (IV)	Screen printed graphite electrodes	19.2 µg L^{-1}	10 to 1000 µg L^{-1}	NA	anodic stripping voltammetry	x	32
Se (IV)	Thick-film-graphite electrodes	0.1 µg L^{-1}	0 to 50 µg L^{-1}	NA	stripping voltammetry	✓	33

sludge with content of Se up to 90 wt.% [9]. In general, wastewaters from different industrial processes [10] could contain a significant amount of Se up to tens of mg L^{-1} ref [11]. Many studies reported that natural selenium concentration is measurable at µg L^{-1} levels in various aquatic sources [12,13]. In some salty lake waters, selenium concentrations of up to 2000 µg L^{-1} have been discovered [14] whereas a dissolved selenium occurrence in natural waters is generally between <0.01 to 100 µg L^{-1} ref [15]. To protect health and control the selenium pollution of water, the chronic aquatic life criterion has been established for total selenium content to 5 µg L^{-1} by the USEPA standard [16]. Drinking water is controlled by the limits which are set to 50 µg L^{-1} by USEPA and 10 µg L^{-1} by the European Commission, which were accomplished by many studies using the different setup for Se determination (Tab. 1) [17–19]. Recently, stricter limits have been set for water lotic and lentic water ecosystems by the US environmental protection agency (EPA) at 3.1 and 1.5 µg L^{-1} (30-day exposure), respectively.

Selenium also enters **air** from the sources such as the combustion of fossil fuels or volcanic eruptions. In the atmospeher, it can bind to the fine dust particles. The most prevalent forms are selenium dioxide, hydrogen selenide, and methyl selenide. The average Se concentration is measurable in µg m^{-3} range [6].

Se in the soil is mainly governed by weathering processes that release about 100,000-200,000 tonnes of Se per year [6]. Another primary source is atmospheric deposition and fertilizers[34]. In the past, Se could be found as a component of pesticides solutions [6]. The distribution is dependent on pH, redox potential, organic matter [3]. For example, in acidic

soils (pH 4.5-6.5), Se occurs in the form of selenite [6] while it forms very mobile selenates in alkaline soils (pH > 7.5) [6].

Many studies estimated that the average selenium level in soil is between 0.01 and 2 mg kg^{-1} in most types of soils [1,6,35], but it can reach as high as 1200 mg kg^{-1} in the seleniferous soils. The most abundant species in soils are selenates which are easily affected by competitive soil ions (K^+, Ca^{2+}, Mg^{2+}, SO_4^{2-}, and Cl^-) in alkaline conditions [36]. Elemental Se occurring in soils can be methylated by microorganisms such as *Aeromonas*, *Flavobacterium*, and *Pseudomonas* to form compounds such as dimethyl selenide or dimethyldiselenide [6]. Other selenium compounds, such as SeO_4 and SeO_3, can also be microbially transformed to SeO_3 and Se, respectively [1]. However, it is very improbable in a water environment where the O_2 and NO_3 are present [1].

Selenium toxicology

Selenium is considered a micronutrient, therefore it can be readily taken up by plants where it enters the food chain in the pedosphere, and it is also accumulated by aquatic organisms (algae, benthic insects, and fish) in a water environment [6,35]. A high amount of selenium could endanger several ecosystems. Generally, highly predisposed to adverse effects are fish species, which suffers spinal and craniofacial malformations [35]. This idea is also supported by the study of Ohlenford et al., who reported the high amounts of bioaccumulated selenium in fish (on average 6-35 mg kg^{-1}) and in mosquito fish (on average 170 mg kg^{-1}) [37]. Other endangered species reported were mammals, birds, and ruminants [35].

Low doses of selenium are necessary for human health because it protects tissues from oxidative damage as a component of glutathione peroxidase (GSHPx) [6,34]. It is also present in peroxidase enzyme deiodinases and thioredoxin reductases [6,38,39]. The Se is presented in these types of enzymes as selenocysteine, a modified amino acid. Selenium toxicity is caused by their reactivity with thiols which reduces the DNA repair ability [39]. Daily intake exceeding 400 µg/day may lead to chronic disease selenosis. Moreover, a high level of exposure via inhalation or ingestion to Se or selenium compounds may cause adverse health effects such as pulmonary oedema, gastrointestinal disorders (nausea, vomiting, diarrhoea, and abdominal pain) and disorders of the nervous system [17,40]. The Se deficiency (<40 µg/day) results in cirrhosis of the liver, carcinoma, and Keshan disease [41,42]. The recommended daily intake for an adult human is 55 µg of selenium per day, which is established by the U.S. Agency for Toxic Substances and Disease Registry [34,35].

Selenium determination

Selenium is determined by well-known techniques such as flame atomic absorption spectroscopy (FAAS) or atomic fluorescence spectroscopy (AFS), in which the concentration of selenium is detectable from 10 mg L^{-1} to 8200 mg L^{-1}, with requested specific preliminary actions. To determine selenium concentrations between 0 and 50 µg L^{-1}, the use of graphite furnace AAS (GFAAS) can be employed [36,40,43], with the addition of platinum matrix modifiers. There are obvious limitations when selenium concentration in the sample is in the range from 0 to 10 mg L^{-1}. Such concentration range requires sample dilution and pre-treatment, which could add significant error into analysis. Alternatively, inductively coupled plasma-mass spectrometry (ICP-MS) is very often used due to the highest sensitivity and the best detection ability near to 0.1 µg L^{-1} [44–46]. However, the instrumental and analysis cost is one of the highest [47]. Other methods reported for selenium determination are gas (GC) and liquid chromatography (LC) [48,49]. Many researchers also applied advanced techniques for improved speciation and detection, such as ion chromatography (IC) and capillary electrophoresis (CE) [50,51].

To overcome disadvantages and limitations of the above-mentioned methods, the use of electroanalytical techniques such as adsorptive cathodic stripping voltammetry (CSV), anodic stripping (ASV) and square wave voltammetry (SWV) should be considered [35,52]. However, it is not always possible to determine all selenium species electrochemically. The pre-treatment step, including preliminary reduction of Se(VI) to Se(IV) using concentrated HCl at high temperature or UV photolysis in alkaline solution (pH value 8.1-8.3), is often needed in order to determine the concentration of both selenate and selenite [35,53]. Generally, these techniques allow determining the selenium content in the environmental samples at the detection limit of µg L^{-1} [53]. For example, in one study, authors modified glassy carbon electrodes (GCE) using gold nanoparticles (AuNP) which provide an enhanced method with the capability of Se(IV) determination with a detection limit of 0.64 µg L^{-1} ref [54]. Moreover, the determination may be influenced by the presence of interfering species such as (Ni, Cd, Cu) [54,55].

On the other hand, there are numerous studies investigating novel materials for sequestration of selenium species from the polluted water with a general focusing on adsorption (or, to be precise, chemisorption) of selenite or selenate on the surface of these materials. The sorption was often achieved with excellent selectivity, under a wide range of pH and diverse levels of reversibility [20,56,57]. The selective adsorption has also been coupled with analytical methods, especially for pre-concentration or speciation of analytes to achieve higher selectivity and sensitivity [58]. It has also been agreed that tailoring of electrodes' surface properties to secure affinity of the analysed species or repel the interfering agents or electrode reaction products is a crucial step towards high-performance electrochemical sensors [28].

The aim of this review is to assess the processes and materials that could be potentially employed for the development of high-performance electrochemical selenium sensors usable for fast and sensitive screening of inorganic selenium in wastewaters, but possibly also in biological samples or natural and tap waters. The first chapter is focused on electrochemical reactions of Se(VI) and Se(VI) on different types of electrodes, that is, reactive and non-reactive and unmodified and modified. This part also shows how electrochemical signals from these reactions can be

amplified by modifications of electrodes either by electrocatalysts or by sorbents to increase selenium concentration on an electrode surface. Employment of a reduction for speciation and electrochemical sensing gain is also covered in this chapter. In the second part, sorption and interaction of inorganic selenium on different types of materials is reviewed, covering separately main types of materials, that is, metal and metal (hydr)oxides, carbonaceous particles, polycations, metal organic frameworks and ion imprinted polymers. Special attention, throughout all the sections, is paid to nanoformulations of adsorbents. The final part summarises the main features of the reviewed materials and discusses their possible applications for the modification of electrodes and the development of inorganic selenium sensors.

2 Redox transformation of selenium

2.1 Electrochemical redox transformation

This section should be opened with a quotation of the 2017 review [39] covering methods for electrochemical determination of diverse selenium species. Of equal significance is the review by Zuman and Somer [59] covering in depth electrochemical behaviour of selenium on different electrode surfaces.

In the latter paper, reduction on "reactive" and "non-reactive" electrodes is distinguished based on whether the electrode material forms a complex with selenium ions or not. Another discerning of redox electrode reactions of selenium can be set between reactions with low-solubility products depositing on the surface and reactions where the products are soluble. This is important, especially in stripping electrochemical methods where typically, in the first step, the electrode surface is covered by insoluble selenium species. This is achieved by the application of deposition potential and followed by voltammetric measurement (square wave, differential pulse…) leading to dissolution (stripping) of the deposited layer. It is therefore reasonable to briefly introduce the main types of reactions that selenium undergoes on different types of electrodes.

2.1.1 Reactive electrodes. Historically, the first electrochemical detection of inorganic selenium was performed on mercury electrode which undergo oxidation to form Hg^+ ions on the surface and consequent formation of mercury selenide [39]. The overall reaction can be approximated as the following two-step reduction:

$Hg + H_2SeO_3 \rightarrow HgSe$ (Se(IV)→Se(0), deposition step) (1)

$HgSe \rightarrow Hg + H_2Se$ (Se(0)→Se(-II), stripping step) (2)

It is important to note that the above detection mechanisms work selectively with selenite ions in acidic solutions. Under these conditions, typical deposition potentials are relatively high, at about -350 mV. The reduction step can be facilitated by the presence of bismuth in the form of $Bi_{(Hg)}$ amalgam. In the deposition step, $Bi_2Se_{3(Hg)}$ is precipitated on the surface of the electrode, which is consequently reduced more efficiently than pristine SeHg [60]. A similar effect could be observed for copper ions which form copper selenide complex which is deposited on Hg electrode. The consequent stripping of $CuSe_{(Hg)}$ provides an increased voltammetric signal over the pristine SeHg [61]. Even higher sensitivity was achieved by adding copper ions and ammonium pyrrolidine dithiocarbamate, which forms a complex with both Se and Cu. This method provided a detection limit of 65 ng L^{-1} ref[62]. The Cu_nSe_n complex is also formed after the electrochemical deposition on a Cu surface, but it was reported that it is more stable than Ag_2Se and AuSe, therefore more negative potential is needed for the consequent reduction [63].

Ag can be employed for electrochemical deposition of inorganic selenium species, with the first such work published in 1996 by Ishiyama and Tanaka [64]. Similar to other reactive electrodes, electrochemical deposition from acid Se(IV) solution leads to the formation of AgSe complex [65], which can be applied in electrochemical selenium sensing [66,67].

2.1.2 Non-reactive electrodes. Like some other elements, selenium can be deposited on different metal surfaces via a process called underpotential deposition (UPD). During this process, metal ions (mostly Se(IV)) are reduced and, in a zero-valent redox state, form a monolayer on a non-reactive metal surface. This process is thermodynamically facilitated; therefore, it occurs at potentials lower than the potential needed for bulk electrodeposition. When the UPD-formed monolayer covers the substrate surface, the deposition potential must be increased to keep deposition of selenium on the formed selenium monolayer [68].

UPD of different species, including selenium, was investigated by the research team of Tedd Lister. More than two decades ago, they described the formation of electrochemical adlayer of Se on gold electrodes (monocrystalic Au(100) [69] as well as Au(111) [70,71] and Au(110) [70]) deposited from an aqueous solution of $HSeO_3^-$. Although UPD-like, the deposition actually occurred at overpotential. This was also observed by Alanyalioglu et al. [71], but they suggested that the observed UPD-like process is, in fact, the reduction of selenate, which has previously and spontaneously adsorbed on the gold surface. The reduction itself was thought to proceed stepwise, that is, Se(IV) + 4 e^- → Se(0) and consequently Se(0) + 2 e^- → Se(-II), but Wei et al. claimed that also direct, six electron reduction Se(IV) + 6 e^- → Se(-II) is possible and occurs as a competitive reaction together with the former one [72]. Later it was reported that UPD of selenium from acidic solution is facilitated when Au electrode was used, compared to Pt (**Figure 2**) [30]. Finally, Pt electrodes provided also an appropriate surface where selenium oxyanions can be reduced [73]. To point out the differences, Beni et al. compared selenium redox changes on gold and platinum disc electrode with results suggesting that, under acidic conditions, two-step deposition (UPD and bulk deposition) of the reduced Se occurs on Au surface

while the first step is omitted on Pt under the same conditions [30].

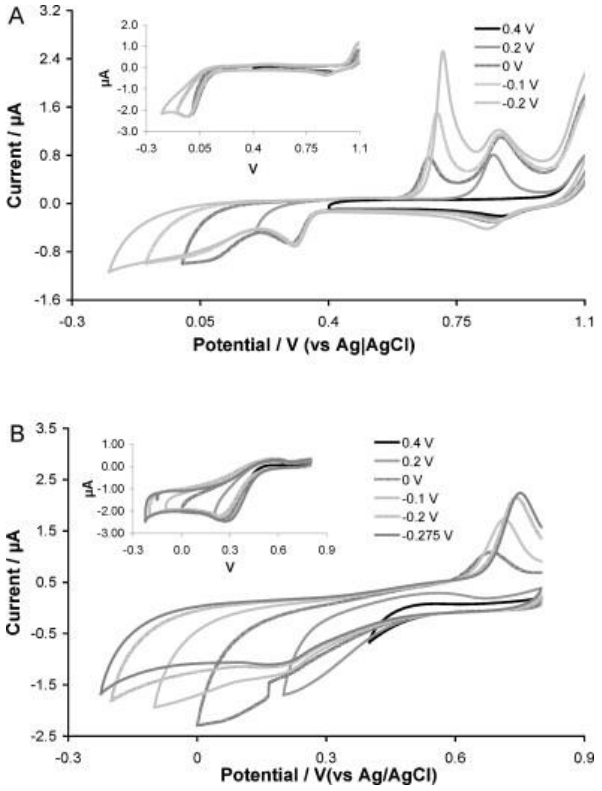

Figure 2: Difference in electrochemical redox behaviour of 0.5 mM Se(IV) on Au (A) and Pt (B) electrodes. Reprinted with permission from Beni et al., 2011 [30], copyright Elsevier 2011.

Another interesting comparison was performed by Ivandini and Einaga who observed clear oxidation and reduction of selenite and selenate on gold-coated boron-doped diamond electrode, but no reaction was observed on pure boron-doped diamond [29]. Gold electrodes have been also employed for determination of Se(IV), as exemplified by a flow-through cell equipped with a gold working electrode [74] or by an older study where Se(IV) from biological samples was deposited on the gold electrode and determined with a help of stripping voltammetry [31]. The performance of such devices further improved upon modification of the electrodes in nanoscale (see **table S1** in electronic supplementary information). For example, electrodes modified by combination of so-called gold nanocages and fluorinated graphene exhibited a synergistic gain in voltammetric response to Se(IV) in acidic solution [42]. Similar synergy was observed on electrode modified with gold nanoparticles and ZnO nanocomposite [75]. The electrochemical reduction of selenium species has been investigated also on other metal surfaces. Se can form adlayers also on Rh(111) surface [76] and indium tin oxide (ITO) was also investigated as a conductive and transparent substrate for selenium electrochemical deposition [77].

Even though noble metals are great electrode materials for, there is an effort to replace them by some cheaper alterntatives. Various carbon (nano)materials are often a first choice mainly because of their relatively low price, easy handling and abundance on market. It was revealed that selenite anions can be at acidic pH also reduced by graphite and glassy carbon electrodes with the main cathodic peaks at about -0.5 and -0.75 V (vs. Ag/AgCl reference electrode), respectively [78]. Also, a carbon paste electrode [79] and cheap screen-printed graphite electrodes [32] can be employed for Se(IV) electrochemical reduction/cathodic deposition. Since graphene introduction in 2006, a great number of studies have appeared investigating applications of this material and its derivatives in, among many others, electrochemical sensing. One of the first work where reduced graphene oxide was deposited on electrode surface for selenite sensing was Idris et al. [80].

2.2 Modified electrodes

As opposed to gain in electrochemical signal achieved by enhanced heterogeneous redox reactions described in the previous subsection, enhanced absorption electrodes relies on fast and spontaneous absorption of selenium species into the matrix deposited on the electrode surface. This amplification method relies on engineered polymers with anion-binding functionalities. For example, electropolymerized diaminonaphthalene (DAN) was used to modify gold electrode and voltammetric determination of Se(IV) species in an aqueous solution with a limit of detection 710 ng L^{-1} [81]. DAN forms piazoselenol-type of bond with Se(IV) (**Figure 3**).

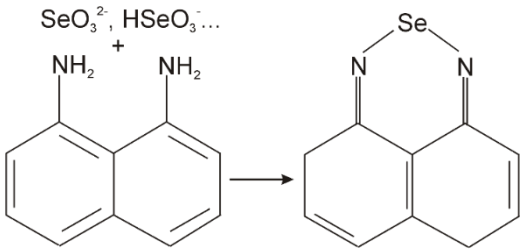

Figure 3: Scheme of reaction of 1,8 diaminonaphthalene with selenite resulting in piazoselenol-type bond.

DAN could be also employed without the immobilization on the electrode. After the addition of diaminonaphthalene into the analysed solution, a complex with Se(IV) is formed, which can be determined electrochemically with higher sensitivity [33]. Derivatives of o-phenylenediamine (OPD; **Figure 4**), that is, 4-nitro-1,2-phenylenediamine [82,83] and 4-methyl-o-phenylenediamine [84] worked in the same way.

A. A. Ramadan´s group investigated voltammetric detection of Se(IV) by series of electrodes modified by nafion (polyanionic polymer) grafted with 3,3´-diamionobenzidine (DAB; **Figure 4**) [85], OPD [86] or methylene blue [87]. All of them were superior over the electrode modified with a composite of Nafion and tocopherol. The latest provided a 10-fold higher detection limit compared to 390 ng L^{-1} achieved with Nafion-methylene blue while DAB- and OPD-based sensors offered LOD of 60 and 48 ng L^{-1}, respectively. However, this is still higher than 20 ng L^{-1} achieved with carbon composite with optimized porosity and modified by OPD [88]. These studies show that amino groups could interact with selenium anions much stronger compared to tocopherol´s hydroxyls. Selenium interacts also with quaternary amines of so-called

room-temperature ionic liquids. Matveichuk reported electrochemical sensing of selenate by electrode modified with 3,4,5-tris(dodecyloxy)-benzyltetroxyethyltrimethylammonium chloride which served as Se(VI) preconcentration matrix [89].

Azizi and Babakhanian [28] modified graphite (pencil) electrodes with electropolymerized poly(pyrrole) containing molecules of acetophenone (2,4-dinitrophenyl)hydrazone (**Figure 4**) which has shown to facilitate the redox transformation of selenium on the electrode. Although relatively high detection limit of 1309 ng L-1 was reached, this work is an example of an amplification mechanism relying rather on electrocatalysis than on absorption /preconcentration.

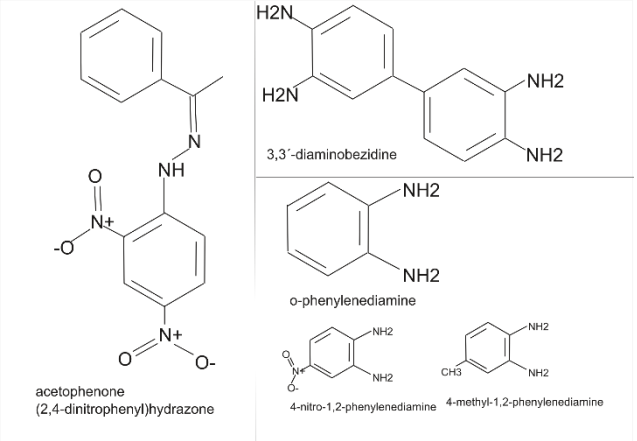

Figure 4: Structures of chemical agents used for complexation of selenium species.

2.3 Reductive speciation

To achieve the reliable information about total inorganic selenium concentration in the given sample, it must be taken into account that the conditions for the determination of individual species (i.e. Se(IV), Se(VI) or zero-valent Se(0) and reduced Se(-II)) may be quite different and that those species often coexist in the sample. Therefore, initial studies on electrochemical detection of inorganic selenium employed sample pre-treatment, e.g. 1-hour incubation with 6 M HCl at 85°C [90] to reduce Se(VI) quantitatively to have only Se(IV) in the sample. The latter anion, as discussed in the above section, can be detected using voltammetric methods. Other commonly used reducing agents include sodium borohydride or hydrazinium sulfate, as reviewed, for example, by Chetna et al. [91]. Some species (borohydride) can reduce selectively Se(IV) to gaseous H_2Se leaving only Se(VI) in the solution [92]. This treatment - selective sequential hydride generation, SSHG – is, in fact, a very common speciation method for inorganic selenium, especially outside the electrochemistry field (see the recent review [55]). UV irradiation is also capable of reducing Se(VI) to Se(IV), which could be employed for speciation [93], as well as hydrochloric acid [94]. Iodide, reducing Se(IV) to Se(0), can be employed for iodometric determination [95]. It should be also noted that Se(-II) generated during cathodic stripping voltammetric analysis (see reaction (2)) is a reducing agent and can be responsible for the spontaneous reduction of Se(IV) to Se(0).

Some studies investigated employment of less toxic and „green“ reducing agents (ascorbic acid[96,97], saccharides and their derivatives [98,99] and other biomolecules [100,101] including plant extracts [102,103]), primarily for production of Se nanoparticles, that is, reduction of Se(IV)(l) to Se(0)(s). Such reduction with precipitation of Se(0) may also be applied for speciation and preconcentration in electrochemical determination as exemplified by Kumar et al. They added sodium borohydride to the solution containing a known amount of Pd(II) and a mixture of Se(IV) and Se(VI) at concentrations to be determined; this addition caused a formation of Pd nanoparticles on the surface of which Se(0) was precipitated, but only from Se(IV) portion, because Se(VI) is under the given conditions reduced only to Se(IV). Thus, by the collection of the formed Pd/Se nanoparticles by centrifugation, Se(IV) can be qualitatively separated from Se(VI) and preconcentrated at the same time [104]. Relatively simpler modification of such preconcentration was introduced by Bertolino et al. who reduced Se(IV) by ascorbic acid in the presence of activated carbon particles, which were consequently collected together with the solid-form Se(0) and further analysed by conventional analytical techniques [53]. It should be noted that when the authors employed “stronger” reducing agent (hydrazinium sulfate), total Se(IV) + Se(VI) could be determined due to the non-selective reduction of both species.

The selenite or selenate reduction to Se(0) or Se(-II) can also be performed by many microorganisms including bacteria *Streptomyces minutiscleroticus* M10A62 from a magnesite mine [105] or *Rhodopseudomonas palustris* [106], yeasts *Saccharomyces boulardii* [107], fungus *Aspergillus oryzae* strain RIB40 [108] and so on. It should be noted that bacteria are also capable to reduce not only Se(IV), but also Se(VI) first to Se(IV) and then to Se(0), which may be applicable for inorganic selenium speciation. Also, a specific reduction of Se(VI) only to Se(IV) was reported, with a mixed bacterial culture [109]. Biological reduction is achieved by diverse enzymes, including cytochrome 3 [110] or metal-dependent selenate reductases [111], sometimes located in the cell such as its active site reaches periplasmic space of bacteria [112].

Electrocoagulation Unlike the voltammetric methods with the signal resulting from the heterogeneous redox reactions on the electrode surface, electrocoagulation relies on the bulk reduction of soluble selenium species to the insoluble Se(0), also driven (or aided, in some cases) by a potential applied between two electrodes. It is mainly used for selenium sequestration, but application in the sensing field should not be ruled out. In simpler electrocoagulation set-ups, Fe(II) ions are electrochemically produced in-situ and are oxidized (by addition of, for example, H_2O_2) to iron hydroxide that readily forms a complex with selenite. Such a method could decrease selenium levels in treated water below the legislation limits [113]. Electrocoagulation performance can be enhanced by ultrasound treatment [114],

which helps to keep the formed iron hydroxide particles separated and prevents their aggregation, or by the addition of zero-valent iron nanoparticles (nanoZVI), as reported by Hansen et al. [115]

3. Interaction of selenium with metal-based (nano)materials

This chapter aims to review interactions of inorganic selenium species with diverse types of metallic materials. These interactions have been studied mainly to i) elucidate occurrences and spreading of inorganic selenium in the environment (interaction with and sorption to minerals) and ii) to achieve sequestration of selenium from waters.

The chapter is opened by the section dedicated to zero-valent iron which provides unique complex interaction ("reactive sorbent") and continues to covering of interaction with diverse types of metal oxides and hydroxides. It should be noted that carbon-based materials/particles enriched with metallic binding sites have not been included in this section.

3.1 Zero-valent iron

Zero-valent iron (ZVI) is commercially available, cheap sorbent, usually used in the form of particles of a size of hundreds of μm. Their applications in polluted and waste water treatment have been and still are very intensively investigated, there seems to be a tremendous range of possibilities offered by chemical and physical properties of ZVI [116,117], including sorption of both selenate and selenite. The adsorption was found to rely on a formation of iron (hydr)oxides on ZVI surface that is responsible for bonding selenite/-ate on the surface. The adsorbed oxyanions are then reduced to Se(0) or Se(-II) – **Figure 5**.

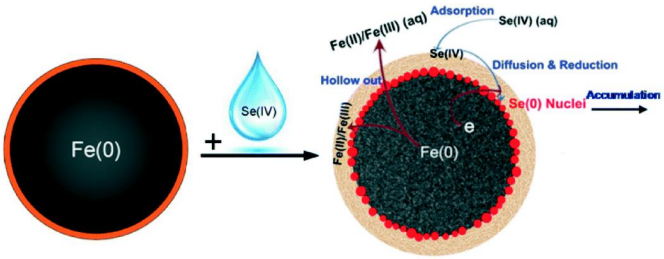

Figure 5: Schematic illustration of reaction of Se(IV) with ZVI particles. Reprinted with permission from Xia et al., 2017 [274], copyright RSC 2017.

The latter step is driven by electron transfer between Fe(0) and selenium species, often hindered by the iron (hydr)oxide film formed on the surface of ZVI particles. Therefore, it is important to reach equilibrium between those two requirements, as evident from optimization studies focused on control of the surface iron hydr(oxide) amount. It is usually achieved by "pre-corrosion" – incubation with an oxidizing chemical agent such as bisulphite, H_2O_2 and other chemicals. Other factors playing a role in the sorption/reduction efficiency are oxygen concentration, potentially interfering ions, and pH change (see **Table S2** in electronic supplementary information). Another way to increase Se sequestration efficiency of ZVI is the simple addition of Fe(II) into the treated solution. It triggers the generation of additional Fe-OOH moieties on ZVI surface leading to more efficient Se(IV) binding and consequent reduction. Such treatment led to 100-180 % increase of Se(VI) sequestration capacity, but only when the solution was aerated [118]. Co^{2+} or Mn^{2+} addition increased the selenium sequestration as well, due to their catalytic effect on Se(VI) reduction and improvement of electron exchange between Fe(0) and selenium anions [119]. Application of ultrasound waves [120] or external weak magnetic field (WMF) [121] has a similar positive impact, partially by mechanical disruption of fouling iron oxide film. The effect of WMF application on Se(IV) sequestration rate (at pH 6) was indeed striking (halve-life of Se(IV) in the treated solution decreased more than 40 times) for 5 mg L^{-1} initial Se(IV) concentration, but it diminished with its increase up to 40 mg L^{-1} of Se(IV) [121]. Importantly, Fan et al. compared all the above-mentioned methods of ZVI enhancement and found that Fe^{2+} addition is the most efficient one, in terms of Se(VI) removal as well as operational pH range broadening (high absorption rate kept up to pH = 9 compared to all other ZVIs that worked well only in acidic conditions) [122]. Integration of ZVI particles into porous support materials can be a reasonable way to improve mass transport in the system and improve Se sequestration and recovery. For example, ZVI particles mixed with so called pillared bentonite exhibited improved Se(VI) sequestration not only because of the above-mentioned gain in mass transport, but also because buffering effect of the bentonite which helped to keep pH at advantageously low level [123].

Application of ZVI in nanoform (nanoZVI) has been considered an important step towards advanced water cleaning process mainly due to large active surface area, good and adjustable electrical and chemical properties and notably low price [57,124]. NanoZVI bind and reduce selenium oxyanions in the same way as ZVI (see **Table S3** in electronic supplementary information), but with increased efficacy. Se(IV) was removed from the solution approximately three-fold faster by nanoZVI than micro ZVI and other sorbents [125]. Reportedly, Se(VI) can interact with nanoZVI too, as exemplified by the four-fold Se(VI) absorption rate by nanoZVI compared to micrometer-sized ZVI [126]. NanoZVI efficiency could be further increased by preoxidation techniques described for ZVI and electrochemically, as exemplified by the recent study of Qi et al. They employed freely dispersed ZVI nanoparticles in a Se(IV)-containing solution with immersed anode and cathode. The applied potential enhanced the nanoZVI oxidation on the anode, which improved absorption of Se(IV), while enhanced Se(IV) reduction to Se(0) occurred on the cathode. The synergy of these reactions led to the sorption capacity of 15.8 mg g^{-1} and improved selenium sequestration by 25 and 127 %, respectively, at anodic and cathodic parts of the cell [127]. Mondal et al. [128] revealed that bimetallic (Ni/Fe with 50-70% Ni) nanoparticles enhanced the reduction rate of Se(VI) by

56% compared to pristine nanoZVI, broadened the operation pH window up to 8 and retained the sorption also in the presence of chloride and nitrates. Presumably, such gain is caused by the high catalytic activity of Ni, which galvanically oxidizes Fe(0) and directly promotes the reduction of Se(VI) to Se(IV) and its consequent adsorption [128].

Higher performance can be achieved when ZVI nanoparticles are anchored to a solid substrate. For example, zeolite or activated charcoal and biochar coated with ZVI nanoparticles (see **Table S3** in electronic supplementary information) exhibited increased Se(VI) adsorption than its counterpart without ZVI nanoparticles. Another example is carbon nanotubes(CNT)/nanoZVI nanoparticles synthesized by Sheng et al., who observed the Se(IV) sequestration by the hybrid nanoparticles was faster than the one achieved with either sole CNT or sole nanoZVI [129]. Other advanced selenium oxyanion sequestration systems are, for example, nanoZVI supported by carbon matrix and porous silica layer [130], nanoZVI entrapped in anion-exchange polymer [131] or nanoZVI deposited on titanate nanotubes where more than two-fold increase in absorption rate was observed, compared to pristine materials [132].

3.2 Metal oxides, hydroxides

3.2.1 Iron (hydr)oxides Originally, geochemists have studied sorption of selenium species on different components of soils – see, for example, the 1987 investigation of Se(IV) and Se(VI) adsorption on geothite (α-$Fe^{3+}O(OH)$) performed by Balistrieri and Chao [133]. Other authors, as listed in **Table S4** in the electronic supplementary information, have further investigated it and revealed that iron (hydr)oxides interact with selenite and selenate ions via different mechanisms [134,135]. In the former case, so called inner sphere complexes are proposed (**Figure 6**), according to Martínez et al. [134]

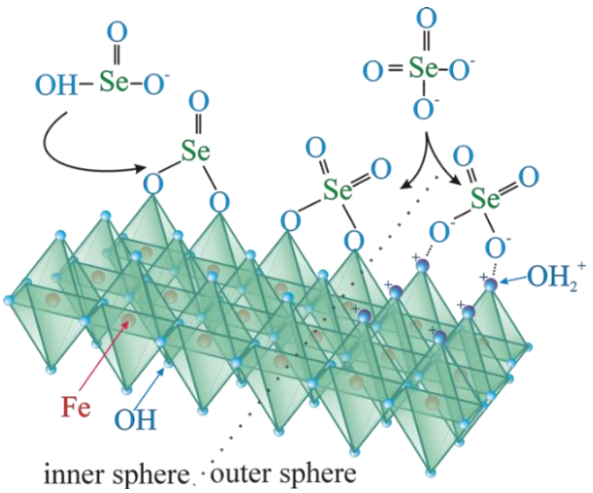

Figure 6: Schematic illustration of bidentate inner sphere complex for selenite (left) and selenate (right), where also the outer sphere complex is illustrated.

Se(VI) is supposed to predominantly bond via outer sphere complex (**Figure 6**) [134], but the inner sphere complexes cannot be ruled out, as suggested by some authors [136]. The bonding type is always determined by parameters including ionic strength, pH, selenium concentration and adsorbent composition. In the important 2018 study [137] it is explained how the nature of selenate bonding to FeOOH changes with increasing pH from monodentate and bidentate inner sphere complex (pH 2) to mixture of inner and outer sphere complex (pH 8) [137]. The recent study of selenate sorption to goethite has confirmed that the sorption rate is promoted with the acidity of the solution [138], as a result of the higher positive net charge of ferrous oxohydroxide [135] (with a point-of-zero-charge above pH of 7). It should also be noted that under the appropriate conditions, the selenium species adsorption is relatively fast and that the difference in the binding mechanism for Se(IV) and Se(VI) results in favoured sequestration of the former oxyanion, compared to the latter [134]. These features make iron (hydr)oxides possible candidates for electrochemical sensors development. Furthermore, the commercially available FeOOH was tested as a facile and low-cost selenium adsorbent for wastewater treatment. For example, Sharrad et al. observed 90% removal of initial 0.05 - 2.0 mg L^{-1} Se(IV) in 1 hour at pH 5 and 26 mg g^{-1} of sorption capacity calculated from Langmuir isotherm model [139]. The sorption capacity can be further increased by tailoring the amount of –OH moieties in FeOOH complex by adjusting the fabrication conditions [135].

Oxidized iron can also be used in the form of nanoparticles in order to increase the active surface area and the sorption efficiency. For example, simple Fe_3O_4 nanoparticles of approximately 25 nm in diameter were found to have a maximum sorption capacity of above 2.4 mg g^{-1} for both Se(VI) and Se(IV) [140] compared to approx. 0.250 mg g^{-1} of hematite [141] or magnetite particles [134] of the size of tenths of μm and <5 μm, respectively. Although such comparisons may not always be very informative due to different experimental conditions, some general statements can be made. For example, the pH profile of Se sorption is quite similar for nano- and micro-formulation of iron (hydr)oxide – the maximum absorption is achieved at acidic pH and at about pH = 5 the sorption efficiency decreased for selenate, while it is retained unaffected for selenite up to pH = 6 [140].

Iron (hydr)oxide nanoparticles can be integrated with some supporting matrix, like the iron-coated granular activated carbon introduced by Ning et al. [142]. They achieved the removal of selenium even from “natural-like” low initial concentration of selenium (1 ppm), and it offered the selenate sorption capacity of about 0.2 mg g^{-1}. Quite impressively, graphene modified with lepidocrocite (FeOOH) showed theoretical absorption capacity of 83 mg g^{-1} [143] and an even higher theoretical capacity of 111 mg g^{-1} was observed when carbon nanotubes modified by iron oxide were used [144]. This value was observed at pH 6 and initial concentration of Se of 1 ppm, which is close to the natural environment.

Inorganic ions (especially sulphates and phosphates) can competitively bind to the sorbents, lowering the selenium sorption rate. On the other side, presence of citric, succinic and oxalic acid has positive effect on sorption capacity as a result of enhanced protonation of the iron (hydro)xide

surface and formation of complexes FeO(SeO)O-CO. But this effect goes hand in hand with a decrease of adsorption rate because the carboxylic acids can occupy the same binding sites as Se oxyanions, although their bond is weaker [145,146]. Furthermore, reduction of adsorbed Se(IV) promoted by oxalic acid and dissolving of goethite with subsequent forming of ferric selenite-like precipitates (citric and succinic acid) may also increase the sorption capacity [146].

This part should be enclosed with a citation of Rao and co-workers' 1996 study where coprecipitation of selenite with iron(III) hydroxide was employed for electrochemical determination of selenium in water samples. The sensing technique relied on mercury drop electrodes and cathodic stripping voltammetry [147], but it can be considered as proof that iron (hydr)oxides can be worthy to scope for more compact and versatile electrochemical sensors development.

3.2.2 Aluminium (hydr)oxides are another potential adsorbents of inorganic selenium oxyanions, although it may not be easy to achieve selective and efficient selenite/selenate adsorption with these materials. Goldberg described the adsorption of selenium on gibbsite ($Al(OH)_3$) and suggested the strong inner sphere complex bond prevailed for both selenite and selenate [148]. But, in contrast to arsenate and phosphate, a certain portion of selenium anions is bound by outer sphere complex, which made the latter two anions competitors for Se oxyanion adsorption [148]. Activated alumina also appeared to provide a surface for selenite/-ate complexation to conclude that sulphate anions bind approximately equally strongly as selenate, which binds less strongly than selenite and molybdate could suppress adsorption of all other anions [149]. In 2008 Su et al. published the speciation profile-based model for surface complexation of Se(IV) on activated alumina showing the complexed -$HSeO_3$ prevailed at pH up to 7 while above this value -SeO_3^- complex prevailed (**Figure 7**) [150]. One of Fe or Al's most significant advantages (hydr)oxides is their abundance and low price. In fact, they can be found also in waste material, as exemplified by Ayala and Fernández, who investigated the adsorption of Se oxyanion on "Bayer electrofilter fines" [151] – the by-product particles from alumina fabrication. Interestingly, they have found relatively unchanging sorption capacity over quite a broad pH range with a significant drop at pH above 10, contrary to other studies reporting the drop of sorption capacity at pH about 6-7 [151].

Efficient Se(IV) and Se(VI) sorption was also described for Al_2O_3 nanoparticles, both freely in solution or confined in chitosan microbeads. The latter formulation increased the theoretical sorption capacity (11.08 and 20.11 mg g^{-1} for Se(IV) and Se(VI), respectively, compared to 10.88 and 9.35 mg g^{-1} achieved with freely dispersed nano-Al_2O_3), but hindered the diffusion process [152]. In another study, Al_2O_3 nanoparticles were modified by dimercaptosuccinic acid to obtain selective sorption of Se(IV) over Se(VI), and it was

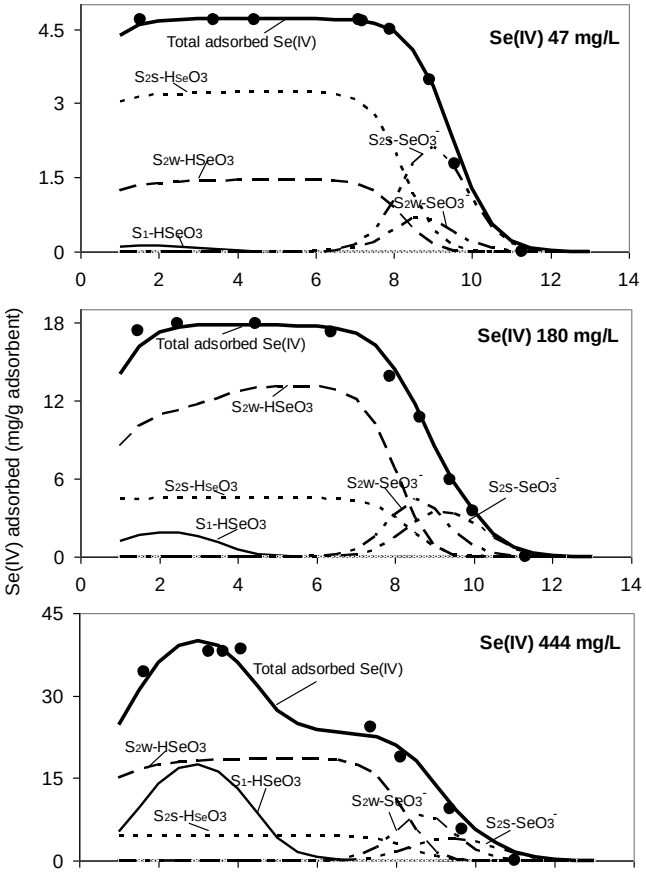

Figure 7: Speciation spectrum of selenite species adsorbed on activated alumina. Reprinted with permission from Su et al., 2008 [146], copyright Elsevier 2008.

combined with nanosized TiO_2 sorbent where both selenite and selenate are captured [153]. Integrated Al_{30} polyoxocations with GO could too interact with selenate with the theoretical maximum sorption capacity of 185 mg g^{-1} at pH 4. But at higher pH and in the presence of phosphates, the sequestration efficacy decreased [154].

3.2.3 Other metal (hydr)oxides In 1997, Davis and Misra published their report on improved Se(IV) adsorption on lanthanum oxide compared to γ-alumina (aluminium oxide) and α-alumina [155]. Also, selenium co-precipitation with $La(OH)_3$ for high-performance preconcentration of Se(IV) has been reported [93]. Interaction of selenium oxyanion with MgO nanosheets was assessed by Cui et al., who observed 103.5 mg g^{-1} maximum sorption capacity for Se(IV) while ten-fold lower capacity for Se(VI) [156]. In 2002, Devoy et al. reported selenite sorption by cuprite (Cu_2O). It was efficient only below pH of approx. 7 and the primary mechanism was the formation of $CuSeO_3$ [157]. Copper oxides have been since investigated, for example again by Devoy and co-workers who confirmed copper selenite precipitation in acidic solution [158]. TiO_2 is another oxide capable of selenite/-ate adsorption [159]. In 2002, Li and Deng reported efficient (concentration factor of 50) preconcentration of Se(IV) and Se(VI) on nanoparticles of anatase (TiO_2 crystal modification) [160]. Svecova and co-workers have performed spectroscopic measurements suggesting that preferentially at lower pH,

complexation of selenium species with the surface $TiO\text{-}H_3O^+$ occurs [161]. Colloidal TiO_2 in the form of nanoparticles dispersion was also found to be efficient Se(IV) adsorbent [24], and it should be noted that titanium dioxide (nano)particles are also commercially available as heavy metal sorbents (Metsorb). It was further developed by adsorption of selenium oxyanions on graphene oxides decorated with TiO_2 nanoparticles (TiO_2/GO) [21], on titanate nanotubes [162] or TiO_2-grafted cellulose fibres applicable for preconcentration and speciation of Se [163]. In all cases, very low retention of Se(VI) on TiO_2 at pH higher than 2 was observed while Se(IV) sorption under less acidic conditions was kept very high allowing for very efficient speciation. The affinity of Se(IV) to metal oxide nanoparticles can be also used directly for Se(VI) or Se(IV) determination. For example Yu et al. have reported metal oxide NPs coated with weakly bounded fluorescence-labelled DNA [164]. These were desorbed from the surface upon the presence of selenite with greater affinity to metal oxide NP and this displacement „switched-on" the fluorescence label on DNA leading to the optical output signal. Notably, authors have assessed a wide range of metal (cerium, indium, niobium, zinc, cobalt, chromium…) oxide nanoparticles to reveal Fe_3O_4 nanoparticles being the best ones for the given purpose [164].

Good results in inorganic selenium sequestration from the water was also achieved with mixed metal oxides. Sun et al. have tested $CuFe_2O_4$, $CoFe_2O_4$ and $MnFe_2O_4$ nanoparticles with results suggesting that all materials adsorbed both selenite and selenate with the capacity of approx. 3-4 mg g^{-1}, only the first two materials were also capable to absorb up to 12 mg Se(IV) per g of $CuFe_2O_4$ or $CoFe_2O_4$ [165]. Chan and co-workers compared two binary oxides, namely Al- and Fe-oxides mixed with SiO_2. They observed that the Al/SiO_2 provides a higher sorption capacity than Fe/SiO_2 for Se(IV) and Se(VI). It is also stated that both species are bonded mainly by inner sphere complex, although their parameters (bond length, bond energy) differs for Se(IV)-Al, Se(VI)-Al, Se(IV)-Fe and Se(VI)-Fe [166]. As an "environmentally-friendly" approach, Thakkar and Mitra used microalgae frustule cell walls enriched with nano-sized particles of zirconium and iron oxide. From Langmuir isotherm, they calculated a maximum sorption capacity of 277 mg Se(IV), but only 0.48 mg Se(VI) per 1 g of sorbent [167].

Se(IV) binding to zirconia (ZrO_2) was reported by Wu et al. [168]. They prepared ZrO_2 porous microspheres sequestering Se from model wastewater in pH range 2 – 10. SeO_3^{2-} bonds to zirconia by kind of ion exchange where surface hydroxyls are released and Zr-O-Se surface complex is formed. Langmuir model revealed a maximum theoretical sorption capacity of 9.5 mg Se per 1 g of zirconia [168]. Rashad et al. used hydrous zirconium oxide and achieved a very promising capacity of 213.2 mg g^{-1} for ^{75}Se(IV) with "most of Se(IV) removed within 5 min" [169] and retained capacity over pH 1.5 – 12, but only for lower Se concentrations (below 1 mM) [169]. Zirconium oxide incorporated into the inner pore structure of Amberlite XAD-7 (crosslinked polyacetate resin) was found to increase the sequestration performance for Se(IV) while negligible Se(VI) adsorption was observed. The binding of Se(IV) is also explained in terms of ligand exchange, that is, oxyanion exchange for complexed water and the sorption capacity of 0.49 mmol (38.7 mg g^{-1}) was observed [170]. In both works, however, significant phosphate anion interference was observed. Also zinc oxide was assessed in selenium sequestration area with a recent contribution represented by Gurunathan et al. [171]. They integrated ZnO nanoparticles (30-40 nm diameter) into cellulose acetate matrix and observed as high as 160.5 mg g^{-1} theoretical sorption capacity towards Se(VI) even at pH 5, which is quite remarkable given the fact that most sorbents exhibited good selenate sorption only at much lower pH [171].

For inorganic selenium immobilization in soils, also alkaline-earth metal oxides (MgO, CaO) were investigated. They enhanced the selenite/-ate immobilization in Fe(II) presence. The proposed immobilization mechanism includes the reduction of selenate (by Fe(II)) and formation of Fe oxide and Ca and Mg hydroxide minerals with a surface suitable for the reduced selenium immobilization [172,173]. On the other side high absorption capacity (103.5 and 10.3 mg g^{-1} for Se(IV) and Se(VI), respectively) was achieved with ultrasonically synthesized MgO nanosheets. It was shown that the sequestration is not very fast (5 h to reach maximum absorption), but it could be performed at quite a high pH (10.5), where most other metal-based adsorbent loose significantly or completely their performance [156].

3.3 Layered double hydroxides

When assembled in layers similar to phylosilicates or clay minerals, metal oxides/hydroxides form structures called layered double hydroxides (LDHs). Their layered nanostructure is similar to clays, but positive charge of M^{2+} and M^{3+} is embedded in the structure imposing the net positive charge suitable for intercalation of anions. The individual layers can be formed by divalent ions including Mg^{2+}, Ni^{2+}, Zn^{2+}, Ca^{2+} and many others and trivalent Al^{3+}, Fe^{3+}, Mn^{3+} and so on, each surrounded by oxygen atoms – see

Figure 8.In 2008 Goh et al. published an exhaustive review covering, amongst other anions, adsorption of selenite/-ate

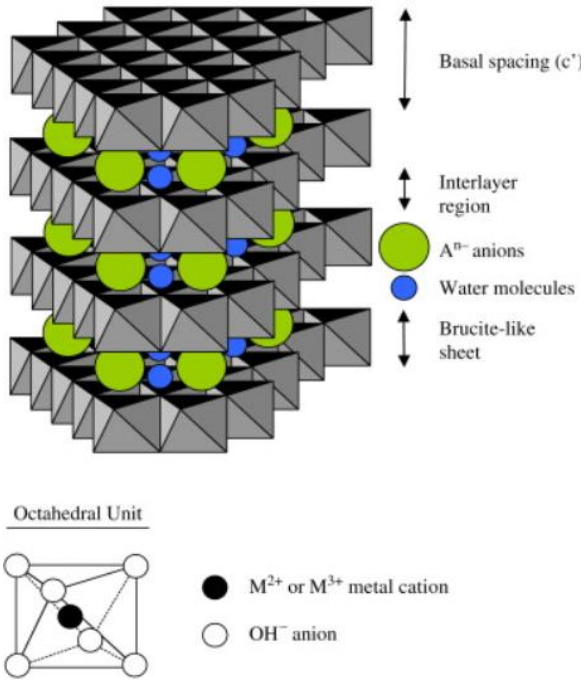

Figure 8: Typical structure of layered double hydroxides. Reprinted with permission from Goh et al., 2008 [174], copyright Elsevier 2008.

on LDHs [174], and selenium sorption on these materials have been investigated by O´Neil et al. since 1990´s [175]. Since then, Mg-Al (most often) or Zn-Al LDHs has been investigated (see **Table S5**). In most studies, competitive sorption of sulphate hindering the selenium sorption was observed, but Chubar and Szlachta [176] introduced the LDH with a structure where the adsorption of both selenite and selenate was suppressed only by some 10% by phosphate and even less by sulphate [176].

LDHs have been prepared also in nanoform, such as hydrothermally treated Mg/Al LDH nanoparticles [177] where hydrothermal treatment substantially increased selenate adsorption by integrating LDH nanoparticles into the chitosan matrix, which decreased the sorption rate. On the other side, homogeneous dispersion of LDH nanoparticles increased the speciation.[178] LDH (Mg-$FeCO_3$) could be grafted on cellulose microfibers where Se(IV) were selectively captured at pH range up to 3.8. Above this pH, also the adsorption of Se(VI) became significant [179]. Notably, Ca-Al-Cl LDH [180] and Ca-Al LDH [181] achieved, respectively, 188.6 and 138.8 mg g^{-1} maximum sorption capacity Se(VI) when removing selenium from caustic wastewaters. It may show how to overcome the problem with a generally low rate of selenium oxyanions (especially Se(VI)) adsorption at higher pH. It was also shown that Mg-Al-CO_3 LDH is capable to capture selenium from wastewaters in a large abundance of sulphates [182]. In the same study, authors claim very fast adsorption of Se(VI) from trace concentration (< 2 ppb) solution, which may be relevant to electrochemical sensing.

"Friedel phases" are Ca,Cl-containig aluminates with properties similar to LDH. Anionic exchange of intercalated chlorides for SeO_4^{2-} can occur at these materials and lead to adsorption capacity as high as 1.37 mmol g^{-1} [183]. Rare-earth hydroxides have possessed even higher anion-exchange capacity compared to LDH [184], but Zhu et al. in 2017 were first to show their applicability also for selenium sequestration in pH range approximately 7 – 9 and in the presence of NO_3^-, Cl^-, CO_3^{2-}, SO_4^{2-}, and HPO_4^{2-}) [185].

To complete the picture, studies should be mentioned where LDHs are integrated with other (nano)materials. For example, LDH and geopolymer were employed for selenite sequestration [186], as well as 2D GO/LDH nanocomposite for adsorption of Se [187]. The latter is very intriguing materials because they possess both negative and positive charge and can be employed for adsorption of both anions and cations at the exact times. These systems were investigated by Koilraj and co-workers, who prepared bifunctional nanomaterial consisting of negatively charged carbon quantum dots integrated with LDH with a positive charge. It could capture both selenium oxyanions and Sr^{2+} cations, which is a needed feature especially for remediation of radioactive wastewaters [188]. In another study, Se(VI) adsorption on LDH integrated with ZVI particles under anaerobic conditions was introduced [189]. This system allowed overcoming passivation problems with ZVI.

3.4 Other minerals/semiconductors

Although selenium species can be reportedly adsorbed on minerals and other compounds occurring in the environment, not many of them were investigated with the same intensity as iron and aluminium (hydr)oxides. Sulphides of different metals are ubiquitous minerals with electrochemical properties of semiconductors. Since selenium has properties similar to sulphur, it is of no surprise that in natural sulphides, substitution of S by Se atoms may occur. Such substitution would require selenium to be in Se(-II) form, which is relatively stable only under specific (reductive) conditions. On the other side, sulphide surface can be oxidized under a wide range of pH [190]. That would lead to the presence of hydroxyls on the surface and selenium adsorption would switch to the scheme described for (hydr)oxides. Naveau et al. suggested that adsorption of Se(VI) on pyrite (Fe_2S) surface is accompanied by redox reaction, namely oxidation of S in pyrite and reduction of Se to Se(-II), with no redox change of the respective cations (Fe…) [191]. However, complexation and/or ionic exchange can also occur, depending on the substrate composition. It is important to note that i) the above experiments were conducted in a non-oxygen atmosphere and ii) the quantitative reduction of all surface selenium species may take a very long time [192]. Such features may not quite meet the demands for fast electrochemical sensing where minimum pre-treatment of sample is requested. In spite of this, Cook et al. have performed experiments where electrodes with microcavity packed with galena (PbS) powder were employed to investigate redox reactions of Se on PbS surface with finding confirming the reduction of

Se(VI) and Se(IV) to Se(0) and, under more reductive conditions, to Se(-II) [193].

Hydroxyapatite (HAp) is a natural form of calcium phosphate, occurring both in rock environments and in living organisms (bone tissue). It was found that selenite can adsorb on HAp (nano)particle surface either by electrostatic interactions (via protonated hydroxyls) or by anion exchange (selenite←→phosphate) and also by surface precipitation by Ca^{2+} ions [194–196]. It was found that the absorption is quite efficient (although the maximum capacity derived from Langmuir isotherm is only 1.9 mg g^{-1} [195]) under acidic conditions, up to pH 6.

3.5 Zeolites, clays

Aluminosilicates, that is, clay minerals and zeolites – both natural (unmodified) or modified – are also capable to interact with inorganic selenium. Unmodified aluminosilicates are formed by structures (planar for clays, 3D for zeolites) consisting of $(SiO_4)^{-4}$ tetrahedrons, $(AlO_6)^{-6}$ (di)octahedrons or their modifications – see **Figure 9**. These structures provide net surface charge, suitable very well for the adsorption of cations under normal conditions. But under strongly acidic conditions hydroxyls can be protonated and sorption of anionic species is possible [197]. Krawczyk-Coda has reported 11 mg g^{-1} of maximum Se(IV) sorption capacity for halloysite nanotubes (basically the rolled aluminosilicate nanosheets) [198]. This was achieved at pH 2 and with the support of ultrasonication. It is higher than for unmodified zeolites prepared from fly ash [199], which could uptake no more than 4.2 mg g^{-1} of Se(IV). For natural clays, it was suggested that Fe, which is often a component of clays, is the main oxyanion-binding moiety and its redox state is strongly dependent on pH and oxygen content. Anoxic conditions have been found slightly more sufficient for selenium sorption on bentonite [200]. Another way to enhance binding of selenite on natural clays is to use high pH solution (above pH of 8) and the addition of Ca^{2+} ions which co-precipitated with SeO_3^{2-} [197].

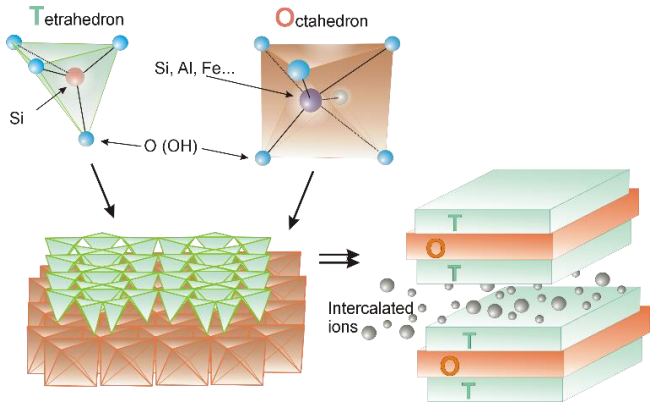

Figure 9: Composition and structural units of clays – tetrahedrons, octahedrons, their assembly in the "T" and "O" layers and typical arrangement of T and O layers in kaolinite.

Another way is the modification of natural clays to switch their net negative charge to the positive one. It was achieved, for example, by hexadecyltrimethylammonium (HDTMA) which reverted the net charge, and such organozeolites could bind oxyanions, including selenite. It could be explained in terms of so-called admicels which are formed when hydrophobic chains of HDTMA molecules in the solution anchor to hydrophobic, out-warding parts of the already surface-attached molecules. Positively charged hydrophilic parts of the outer-layer molecules are then freely exposed to the solution, ready to bind anions (**Figure 10**) [201]. Behnsen and Riebe have assessed the modification of

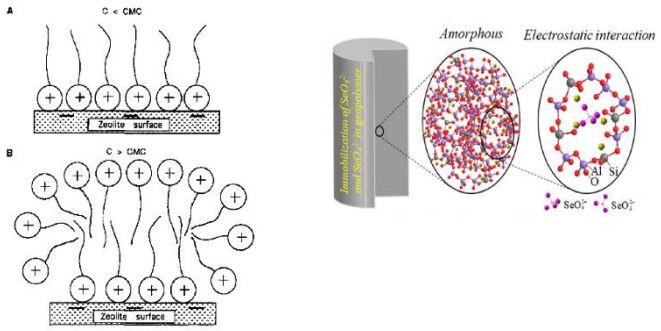

Figure 10: Schematic illustration of (left part) zeolite modified with HDTMA molecules in (A) subcritical micellar concentration and (B) higher than critical micellar concentration when admicelles are formed. Reprinted with permission from Haggerty and Bowman, 1994 [201], copyright 1994, American Chemical Society. The right part – scheme of a structure of geopolymer with the captured selenium oxyanions. Adapted with permission from Tian et al., 2020b [208], copyright Elsevier 2020.

bentonite MX-80 by hexadecylpyridinium, hexadecyltrimethylammonium and benzethonium, but their assumption was that organoclays exhibited poor selectivity towards selenite [202]. In 2004 Saha et al. investigated the kinetics of selenite adsorption on montmorillonite intercalated with different hydroxyaluminum (HyA) and hydroxyaluminumsilicate (HAS) species [203]. They assumed that Se(IV) adsorption rate is significantly increased by the addition of HyA, but suppressed when HAS was used for montmorillonite intercalation [203]. A similar assumption was also made by Haciyakupoglu and Orucoglu, who found the best sorption properties on bentonite modified by the mixture of aluminium hydroxides and organic modifiers over unmodified or only organic-modified bentonites [204,205]. Later, Bleiman and Mishael reported 18.4 mg g^{-1} capacity for adsorbent prepared by mixing of montmorillonite and chitosan [7]. It was surpassed by 112.5 mg g^{-1} of maximum sorption capacity of FeOH-modified bentonite reported by Wang et al. [206]. Recently, Phanthasri et al. observed enhanced Se(VI) adsorption on zeolite-supported nanoZVI with increased sorption kinetics than unsupported nanoZVI and pristine zeolite [207]. Selenium could also be electrostatically captured into geopolymer – a material similar to clay but more amorphous (**Figure 10**) [208].

4. Interaction of selenium with carbon-based (nano)materials

In this chapter, interactions of inorganic selenium are reviewed with carbon-based materials. These include carbon micro and nano-particles, either bare or modified (e.g. by metal oxides). The second category includes polymers, specifically polycations with different functional groups (nitrogen-, sulphur- and oxygen-based) and polymers with embedded "free-standing" ligands without chemical bond to the polymer backbone. Macromolecules with integrated metallic binding sites and so-called ion-imprinted polymers are the last categories of materials covered in this chapter.

4.1 Carbon micro- and nano-particles

"Biochars" are organic materials with high porosity, large active surface area prepared from organic matter by pyrolysis [209]. The presence of negatively charged moieties, typical for many carbonaceous particles, does not favour the direct sorption of selenium oxyanions. To overcome this, Peräniemi et al. performed sintering of carbon particles with metal salt. Such prepared carbon loaded with zirconium could very efficiently, promptly and reversibly adsorb both Se(IV) and Se(VI) oxyanions from aqueous solution at broad range of pH (up to 10) [210]. From a wide range of metals applicable for such modifications, Fe, Al, In and Hf showed the best results in terms of selenium sequestration [211]. Cu-modification could also be employed for this type of carbon particle modification with a reported theoretical maximum sorption capacity of 4.8 mg Se(VI) per g of activated carbon soaked with Cu [212]. Zhang et al. have confirmed that Se(IV) bond to iron-modified activated carbon is stronger compared to Se(VI). Nevertheless, the difference was not very high (80% versus 97% removal of Se(VI) and Se(IV), respectively) [213]. In 2015 Roberts et al. reported 2.6 mg g^{-1} sorption capacity (Se(VI)) for $FeCl_3$-treated biochar derived from seaweed waste biomass in a pH window of 2.5 – 8 [214]. Even higher capacity was achieved with biochar sintered with $Fe(NO_3)_3$ - 14.3 mg g^{-1} achieved at optimum pH = 5, but sustainable during relatively broad pH range (approximately 2 – 6) [215]. Dobrowolski and Otto reported efficient sequestration of Se(VI) at an even broader pH range (approximately 1 – 11), achieved with activated carbon with an optimised amount of $Fe(NO_3)_3$ during the sintering [216]. Similar $FeCl_3$-impregnated biochar from food waste reached almost 20 mg g^{-1} capacity due to the mathematical optimization of preparation parameters. However, the significant and steady decrease of the capacity with increased pH (from 3 up to 11) was observed [25]. Quite an improved performance was achieved by Johansson et al., who prepared Fe-biochar from algae and achieved Se(VI) sorption capacity of up to 38.8 mg g^{-1}. Notably, this value was achieved in the presence of other anionic species [217]. The same research group has also found a negligible influence of NO_3^- ions, although SO_4^{2-} ions were found to compete with Se(VI) for binding sites. The reason is a different binding mechanism of nitrates compared to selenates and sulphates [218].

Absorption of Se(IV) on biomass-derived sorbents without the precipitated metal oxides were also investigated. El-Shafey employed sulphuric acid-treated rice husk for this purpose and revealed the highest sorption capacity at pH = 1.5 and its significant loss with increasing pH [219]. Baker's yeast waste biomass provided a relatively high maximum sorption capacity of Se(VI) 39 mg g^{-1} at optimum pH=5 [220]. Recently, Dev et al. employed microparticles prepared from air-dried citrus peel encapsulated in alginate beads. To ensure the protonation of abundant –OH groups, which turned them to positively charged moieties, citrus peel microparticles were treated by HNO_3. Theoretical sorption capacity of 112 mg g^{-1} was achieved, but only in quite a narrow pH region, that is, around pH = 6 [221]. Amine moieties-rich biomass, especially chitin parts of crustacean bodies, could also be employed. Niu and Volesky employed waste crab shells which offered a capacity of slightly above 10 mg g^{-1} at pH 3 [222].

4.2 Polycations

4.2.1 N-containing polymers Ionic polymers are materials capable of noncovalent electrostatic interaction with negatively charged selenium and other species. Sulfonated cross-linked polyethyleneimine where positively charged moieties are attached to the backbone can be a good example [223]. Ion exchange resins provide similar function – for example, polyamine resin "Eporasu K-6" which is weakly basic and provided an adsorption capacity of 134 mg g^{-1} [224] or alginate-PEI polymer matrix with the maximum sorption capacity of 83 mg g^{-1} (Se(VI), pH 2) [225]. It should be noted that the sorption is fully reversible (just by pH change) and that the reduction of the attached Se(VI) by the alginate´s hydroxyls and PEI´s amines has occurred. Recently, Min et al. synthesized nanostructured particles from amine-crosslinked organosilica exhibiting excellent polycationic properties as well as sufficient porosity suitable for selective Se(VI) adsorption in a broad pH range [226]. The reported sorption of Se(IV) on poly(1,8-diaminonaphthalene) required strong acidic conditions and was secured by electrostatic interactions provided by $–NH_2$ moieties or piazoselenol-type binding (**Figure 3**) [227]. This type of bonding formed also during sorption of Se(IV) on diaminonaphthalen-coated electrode [81] introduced in the section 2.2.

Another polycation with the positive charge imposed by amine groups is chitosan [228]. It is an abundant and cheap biopolymer that, in the form of relatively large particles, was shown to absorb Se(VI) directly from the solution up to a maximum capacity of 11.8 mg g^{-1} [222]. It also helped increase the efficiency of both Se(VI) and Se(IV) when integrated in a filtration membrane [229]. Nevertheless, the results suggesting that chitosan hindered the selenium sorption rate when used as a nanoparticle binder (Al_2O_3[152] and LDH[230] nanoparticles in chitosan matrix) should be kept in mind.

Quaternary ammonium salts with positive electrostatic charge grafted on the nanostructured substrate are another option. Some of them are commercially available ion-

exchange resins, for example Amberlite IRA-900 with a chloride ion to be expulsed upon SeO_4^{2-} electrostatic binding [231]. The issue here is an intense competition of SO_4^{2-} ions that significantly decrease the sorption capacity for Se. Another problem is the slow diffusion of selenium species into the porous structure of the resin, making the absorption rate of Se(VI) relatively low. On the other hand, He et al., 2016, synthesized polymeric tetrahedral structures with multiple $–NH_3^+Cl^-$ moieties and applied them in a thin nanofiltration membrane with almost 97% retention efficiency toward Se(VI) [232].

Interestingly, slightly lower rejection was observed for Se(IV), which is explained on the base of pH-driven speciation favouring divalent Se(VI) oxyanion over the mixture of divalent SeO_3^{2-} and monovalent $HSeO_3^-$. Quaternary ammonia salt can be used also for modification of nanomaterials, as exemplified by Nyaba et al. [22]. They grafted room temperature ionic liquid (RTIL) "Aliquat 336" on alumina nanoparticles and used them for solid phase microextraction of Se(IV). They have observed that almost none Se(VI) adsorbed on the investigated nanoparticles at pH above approximately 3 while up to pH 7 almost quantitative adsorption of Se(IV) occurred [22].

Nitrogen heterocycle compounds should be also considered here because they can provide positive charge when protonated. For example, Guleria et al. used imidazolium-based room RTIL for reduction of Se(IV) and formation of Se nanoparticles [233]. Awual et al. modified mesoporous silica with diaminohydroxypyrazole derivative (DSDH) and claimed that at pH = 2 the adsorption of Se(IV) was very fast, selective and reversible, but not many details have been provided on the role of imidazole moiety in the claimed formation of the Se-DSDH complex [20]. Nitrogen heterocycles have been employed also for the synthesis of ion imprinted polymers (see section 3.3.5), typically as ligands for Se(IV) complexation.

4.2.2 S-containing polymers

Thiol moieties can interact with selenium oxyanions forming primarily $RS\text{-}SeO_2^-$ structures which may undergo further reactions [234]. Hence Se(IV) could be entrapped into the matrix of cellulose grafted with thiomaleic acid [235] or thioglycolic acid [236,237]; in the former case, the authors claimed that –SH and –OH moieties are responsible for selenium oxyanion complexation, as deduced mainly from FTIR spectra. Even though this system may not look very robust and efficient, the authors claimed 100 mg g^{-1} sorption capacity for Se(IV), at pH 4.5 (70 mg g^{-1} for Se(VI) at pH 0.5) and good resilience against interfering anions. Silica gel could be modified with thiol groups as well, but Se(IV) sorption of this material occurred for pH not higher than approximately 5 [238]. L-methionine grafted on a glassy substrate is another simple material with reported capability to Se(VI) adsorption with complimentary reduction [239].

The sorption of selenium oxyanions on a solid substrate can be enhanced also in different way, that is, specific agent is added to the treated solution, and the formed selenium complex adsorbs very efficiently on a selected substrate. To achieve this, ammonium pyrrolidine dithiocarbamate (APDC) have been employed; the formed APDC-Se(IV) complex could easily adsorb on unmodified nanosilica [240] or graphene nanoparticles [241].

An unprecedentedly high theoretical sorption capacity of 833.3 mg g^{-1} was reported by Gezer et al. with the employment of simple thiourea-formaldehyde resin (**Figure 11**) [242]. Reportedly, the sorption was accompanied by Se(IV)/Se(VI) reduction to Se(0), by freely available =S moieties. Sulfosalicylic acid grafted on silica-coated iron magnetic nanoparticles is also capable of Se capture. Even though it occurred without discerning its redox state, the absorption was very fast – approx. 95% of Se(IV) in one minute when ultrasound was applied to the system. Without the ultrasonic treatment, from 30 ng ml^{-1} Se solution, between 75 and 80 % adsorption was observed for both species [243]. 2003 study by Sahin et al. reported on mercapto-silica (silica gel particles grafted by 3-mercaptopropyl-trimethoxysilane) capturing selectively Se(IV) while leaving Se(VI) in the solution in pH range up to 9 [244]. Contrary to the above-mentioned simple adsorbents, Warkocki et al. [245] synthesized $TiO_2\text{-}SiO_2$ nanotubes grafted by diphenylthiocarbazone molecules, which possessed i) SeO_3^{2-} complexing and ii) photoactive function. These were integrated with the device to selectively capture selenite and simultaneously provide the optical signal correlated to its concentration. Furthermore, the embedded TiO_2 could produce reactive oxygen species upon exposure to UV light, which was employed to recover active sites of the nanomaterial [245].

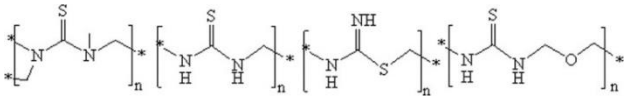

Figure 11: Structural units found in thiourea – formaldehyde resin. Reprinted with permission from Gezer et al, 2011 [238], copyright Elsevier, 2011.

4.2.3 Hydroxyls, zwitterions and ligands

Branched grafted (co)polymers, including polystyrene-g-polyoleic acid-g-polyethylene glycol, are also selenium oxyanions sorbents. Acikkapi et al. [246] grafted such copolymer with precipitated iron oxide to cast magnetism to the polymer matrix. Interestingly, the selenium sorption occurred via amine groups in the employed polymer matrix, but without further clarification which component is the amine-bearing one. Se(VI) sorption was observed also on cellulose-agar blends where only hydroxyl moieties are available for binding occurring after protonation (in an acidic environment) to $–OH_2^+$ [247]. It is of no surprise that such electrostatic attachment is not very strong ($HSeO_4^-$ anions are readily replaced by other ions), nor possessed a high sorption capacity (7.1 mg g^{-1}) or stability [247].

Questions remain on an employment of zwitterionic copolymers bearing both negative and positive moieties. He et al. [248] employed such copolymer to modify the filtration membrane and observed almost quantitative rejection of selenite and selenate from the water passing through the

membrane. Negatively charged moieties in the described system would undoubtedly contribute to the retention of Se oxyanion by their repulsion rather than by their adsorption, therefore its application in possible electrochemical selenium sensing where adsorption would be required is of question.

For Se sequestration also some covalently bound complexing agents are available. Firouzabadi and co-workers reported magnetic carbon nanotubes grafted by "bismuthiol II" (commercially available agent for complexation of Se, Te, Bi) as an efficient preconcentration and speciation nanomaterial [249]. Selective Se(IV) retention was achieved also with "AnaLig As-01" [250] – a commercially available solid phase extraction system with supramolecules designed to capture As-type oxyanions grafted on silica or polymer substrate. However, the calculated sorption capacity of only 11.8 mg g^{-1} was reported [250].

4.3 Polymers with metal atom binding centres

In metal-integrating polymers, positive electrostatic charge results from metal atoms complexed by the polymer functional moieties. Hence, these types of matrixes combine adjustability and versatility of polymeric matrixes and efficient oxyanion binding. As soon as in 2000, Suzuki et al. [251] investigated polymer resin matrix with embedded Zr(IV)-EDTA moieties for Se(IV)) adsorption (see **Figure 12**). Later, Yokoi et al. [252] prepared mesoporous silica substrate modified by amine ligand with coordinated Fe^{3+}. This material was capable of selenate adsorption, but with less efficiency compared to sorption of other oxyanions [252]. Yoshitake and Otsua fabricated similar particles, only Cu^{2+}-coordinated [253]. They also observed selenate adsorption, but a more intriguing study is the one by Yamani et al. [254], who crosslinked chitosan with Cu(II). It was found that where the chitosan-Cu-chitosan arrangement was formed, Se(VI) was preferentially bond to Cu, but chitosan-Cu^{+} moieties (also present in the prepared nanomaterial) offered preferential site for phosphate. Thus, PO_4^{3-} has not concurred to selenium which resulted in practically unaltered adsorption of Se(IV) even in four-fold excess of phosphate in the solution [254]. Quite oppositely, Fe_3O_4 nanoparticles integrated with chitosan have neutralized $–NH_3^{+}$ groups making them unavailable for selenate, but it was overweighed by the increased sorption on the iron oxide nanoparticles [255]. Takada et al. have synthesized micelle mesostructures assembled from hydrophobic chains caped with zirconium sulphate head. These moieties provides ion-exchange sites for adsorption of $HSeO_3^{-}$ with the observed sorption capacity of 195 mg g^{-1} [256].

Besides the above-mentioned "simple" polymers, so-called metal-organic framework (MOF) can be used – supramolecular structures possessing freely exchangeable anions bonded by ligand metal cations (see **Figure 12**). Higher selectivity of MOF towards different ionic species capture is mostly achieved by the precise secondary structure tailoring (the "organic framework" part of MOFs). Stability over a large pH range is another advantageous feature of MOFs.

A recent (2020) review [56] has covered employment of MOFs for extraction of toxic species, including selenite/ate anions, from water. One of the first reports of MOFs employed for selenium adsorption is by Howarth et al. [257] who assessed several Zr-based MOFs and the best one exhibited maximum sorption capacity of 95 and 85 mg g^{-1} for selenite and selenate, respectively. Furthermore, this maximum sorption was reached as fast as within 1 min. Later, by changing the organic framework (from „NU-1000" to „MOF-808"), the same group increased the maximum sorption capacity to 133 and 118 mg g^{-1} for selenite and selenite, respectively [258]. Wei and co-workers have shown that Zr-based MOF exhibit the pH profile of adsorption similar to that described for metal oxides, that is, selenate ions adsorb well only at acidic solutions while, with increased pH, its adsorption capacity steadily decreased. Selenite, on the other side, exhibit the sorption maximum at about pH = 7. It was also found that selenate is more prone to interference by another ions, while selenite exhibited some significant interference only from phosphate [259]. Besides Zr, other metals were also used in MOF, for example, Ni(II)-containing MOF with sulphate anion exchangeable for SeO_4^{2-} was reported to possess the

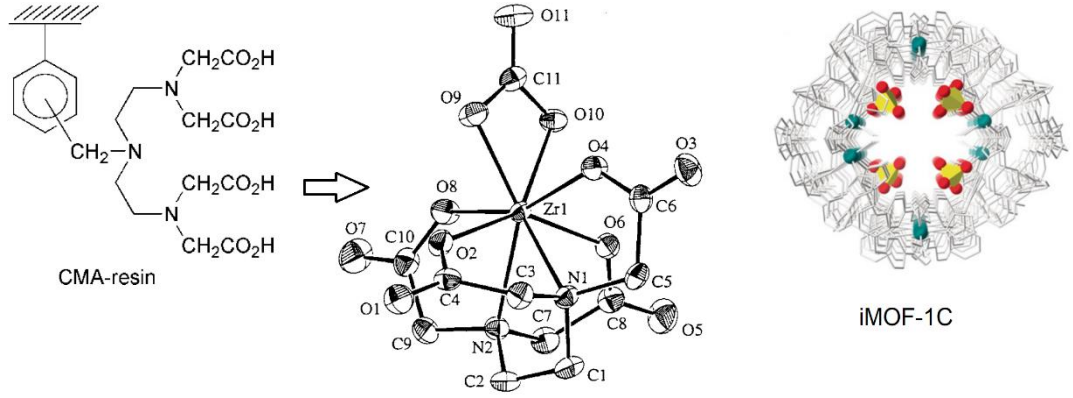

Figure 12: Left - schematic structure of "CMA resin" and its transformation into Zr(IV)-EDTA-modified resin. Adapted with permission from Suzuki et al., 2000 [251], copyright RSC 2000. On the right is structure of iMOF-1C metal organic framework with exchangeable SO_4^{2-} anions shown in yellow and red. Reprinted with permission from Sharma et al., 2020 [260], copyright Wiley 2020.

sorption capacity of 100 mg g^{-1} [260]. Although it is quite a satisfying value, it is not clear whether the initial adsorption phase is fast enough. Li et al. [261] have chosen a structural approach to increase MOF´s capability to Se adsorption up to almost 90 mg $g^{-1}$by the increasing number of structural defects. However, the temporal profile of the adsorption was not very encouraging; it took five minutes to achieve approximately 10 mg g^{-1} Se loading. Further improvement in the sorption capacity (255.3 mg g^{-1}) and kinetics was achieved by the employment of bismuth-containing MOF [262]. To harness both MOFs and nanoparticles´ advantages, Kalantari and Manoochehri [263] synthesized magnetic nanoparticles grafted with dithtiocarbamate to achieve high affinity towards selenium. These nanoparticles were integrated into a structure of chromium-containing MOF and employed for selenium preconcentration. Such an approach helped decrease the limit of detection down to 10 ng L^{-1} and provided a theoretical maximum sorption capacity of 197 mg g^{-1}. It should be also noted that at pH higher than 4 Se(IV) sorption is completely preferred over uptake of Se(VI) [263].

4.4 Ion-imprinted polymers

So-called ion imprinting is the way to achieve very high selectivity. This technique relies on the synthesis of a polymer matrix with embedded ions of interest. After their displacement (e.g. by leaching), a matrix with precisely shaped binding sites remains. The first ion-imprinted polymer fitted for selenite adsorption was synthesized by Khajeh et al. [264] who relied on copolymer matrix containing o-phenylenediamine and 2-vinylpyridine complexing Se(IV) ions during the polymerization. They were leached by 2 M HCl, leaving the material with a good Se(IV) sorption capacity and selectivity [264]. Later, Shi et al. [27] employed sol-gel method for the synthesis of ion-imprinted polymer grafted on silica nanoparticles. They observed efficient Se(IV) uptake even at 50-fold excess concentration of phosphate or sulphate, which is a very notable achievement [27]. The imprinted polymer prepared from 4-vinylpyridine and 1-vinylimidazole in the presence of SeO_2 was employed for preconcentration in Se(IV) detection step [265]. The authors of the study pointed out to the fact that the selenium ions are reduced to Se(0) when complexed in the polymer matrix, hence they propose the term “atomically imprinted polymers” as opposed to previously coined terms ion- or molecular- imprinted polymers .

5. Conclusion, outlooks and perspectives

Sensitive electrochemical determination of inorganic selenium has been achieved with different types of electrodes, including reactive ones (mercury, silver, bismuth, copper) which forms a complex with selenium. Their application brings some disadvantages, especially concerns about mercury toxicity, therefore, some alternatives were sought. Unmodified metal electrodes provide higher stability but, due to their non-reactivity, could not typically offer as high performance as the reactive ones.

As outlined in chapter 2.2, recent research brought some high-performance electrochemical sensors comprised of an electrode modified such as to achieve high affinity to the desired selenium species, allowing for their concentration on the electrode surface. For this purpose, organic molecules with amine functionalities (especially o-phenylenediamine and its derivatives) seem to be very efficient because they provided limits of detection in units or tens of ng L^{-1}. These levels are comparable to convention analytical methods (atomic or mass spectrometry, gas chromatography or their combination) that require expensive equipment. This fact legitimizes the review of molecules or particles that may be employed to modify electrodes to achieve further progress in the development of robust, compact and cheap sensors for inorganic selenium.

Chapter 4 have shown that there is a vast number of materials with the primary purpose of selenium sequestration and with a large capacity to bind inorganic selenium species under diverse conditions and with a diverse range of selectivity. Especially engineered polymers bearing amine- or thio- functionalities seem to be great candidates for the suggested repurposing and application as the preconcentration matrix on the electrode surface. It is further encouraged by the reported maximum adsorption capacity which can easily exceed 0.1 g of selenium per 1 g of sorbent (for comparison see the **Figure S1** in supplementary information file). In addition, ion-imprinted polymers or metal organic frameworks offer great adjustability of properties which is a key factor for the fabrication of highly selective sensors. Furthermore, MOFs can be and have been many times used for the modification of electrodes in electrochemical sensors [266–268]. While most of the mentioned materials can be applied as electrode surface-coating films, it was also shown that many polymers could coat the surface of nanoparticles (e.g. silica nanoparticles) which increases the active (sorption) surface. It can be expected that modification of electrodes with integrated functional coating and structural nanoscale substrate is about to bring the most interesting results.

Chapter 3 have shown that metal-based particles (and nanoparticles) exhibit also interesting properties in terms of sorption of selenium oxyanions. Their characteristic feature is presence of oxygen moieties responsible for selenium binding. There are two issues connected with this type of complexing: 1) oxygen moieties density can be controlled by a simple electrochemical procedure that would expectedly enhance selenium sorption on electrode modified by metal oxide (nano)particles; 2) interaction of selenium oxyanions with the binding moieties of metal oxides is sensitive to the environment conditions - especially pH and presence of competing oxyanions (especially SO_4^{2-}). It will probably make sensors employing metal oxides as the sorption/concentration material assumingly less robust than the ones employing organic modifiers. Not to mention that average reported maximum sorption capacity of typical

metal oxide sorbents is quite low – typically about ten or tens of mg of selenium per 1 g of sorbent (**Figure S1** in Supplementary information file). Notably, this does not imply specific metal-based materials – layered double hydroxides. Their maximum sorption capacity can exceed the one of conventional metal (hydr)oxide particles as high as ten-fold. Furthermore, they can be synthesized relatively cheaply and do not require any rare metals. Hence it seems very reasonable to use them as modifiers of electrodes for high-performance inorganic selenium sensing.

It should be also mentioned that metal oxide particles have been already employed for electrode modification [269–271], justifying the presumption they could be used also for inorganic selenium sensing. The same implies also for LDH [272,273].

Another way of amplification of electrochemical signal of inorganic selenium sensors relies on electrocatalysts. First, it was found that noble metal nanoparticles deposited on electrodes may facilitate redox reactions of selenium ions, making their detection more sensitive. Next, certain selenium complexes exhibited facilitated redox reactions compared to pristine selenium anions. This is the principle of initial polarographic determination of selenium using mercury electrode and it has been also employed with the employment of organic complexing agents. Although it was shown (chapter 2.2) that these complexes were mostly prepared in the electrolyte solution, there are also few studies with complexing agent immobilized on the surface of the electrode.

Complimentary reduction of Se(IV) or Se(VI) was claimed to occurs with binding to =S functionalities. It can be therefore considered that both reduction and preconcentration will undergo on the surface of the electrode modified by this type of functionalities. In this case, no previous electrochemical deposition would be required, unlike for most common electrochemical stripping voltammetry measurements.

As the last concluding remark, it should be noted that throughout the text, hybrid (nano)materials for interaction with the inorganic selenium are mentioned. The possibility of combining properties of different materials further broaden the applicability of the reviewed materials in electrochemical sensors with properties tuned to achieve the highest performance.

Author Contributions

JF – Conceptualization; Writing – original draft
ŠV – Writing – review & editing
EČ – Investigation (literature research)
JS - Writing – review & editing; Formal Analysis

Conflicts of interest

"There are no conflicts to declare".

Acknowledgements

The authors would like to acknowledge the Czech Science Foundation GACR (grant 20-27735Y) for funding this work.

Notes and references

1 P. Neupane, R. T. Bailey and S. Tavakoli-Kivi, *Sci. Total Environ.*, 2020, **738**, 140318.
2 S. Sakan, N. Sakan, I. Anđelković, S. Trifunović and D. Đorđević, *J. Geochemical Explor.*, 2017, **180**, 24–34.
3 S. Etteieb, S. Magdouli, M. Zolfaghari and S. Brar, *Sci. Total Environ.*, 2020, **698**, 134339.
4 L. C. Tan, Y. V Nancharaiah, E. D. van Hullebusch and P. N. L. Lens, *Biotechnol. Adv.*, 2016, **34**, 886–907.
5 P. Kumkrong, K. L. LeBlanc, P. H. J. Mercier and Z. Mester, *Sci. Total Environ.*, 2018, **640**–**641**, 1611–1634.
6 Agency for Toxic Substances and Disease Registry (ATSDR), 2003, 418.
7 N. Bleiman and Y. G. Mishael, *J. Hazard. Mater.*, 2010, **183**, 590–595.
8 V. Bednarik, S. Vinter and D. Nohalova, *Waste forum*, 2015, **1**, 4–10.
9 G. Zha, B. Yang, H. Luo, D. Huang, W. Jiang, B. Xu and D. Liu, *Sep. Purif. Technol.*, 2021, **266**, 118536.
10 O. Otsuka and M. Yamashita, *Hydrometallurgy*, 2020, **197**, 105470.
11 S. Santos, G. Ungureanu, R. Boaventura and C. Botelho, *Sci. Total Environ.*, 2015, **521**–**522**, 246–260.
12 P. Neupane, R. T. Bailey and S. Tavakoli-Kivi, *Sci. Total Environ.*, 2020, **738**, 140318.
13 D. H. Moon, D. G. Grubb and T. L. Reilly, *J. Hazard. Mater.*, 2009, **168**, 944–951.
14 F. M. Fordyce, ed. O. Selinus, Springer Netherlands, Dordrecht, 2013, pp. 375–416.
15 N. Y. V. and L. P. N. L., *Microbiol. Mol. Biol. Rev.*, 2021, **79**, 61–80.
16 U.S. EPA, *Epa 822-P-14-001*, 2014, Office of Water, Washington, D.C.
17 D. H. Moon, D. G. Grubb and T. L. Reilly, *J. Hazard. Mater.*, 2009, **168**, 944–951.
18 U.S. EPA, *Epa 816-F-09-0004*.
19 The Council of the European Union, *Off. J. Eur. Communities*, 1998, L 330, 32–54.
20 M. R. Awual, T. Yaita, S. Suzuki and H. Shiwaku, *J. Hazard. Mater.*, 2015, **291**, 111–119.
21 Y. Zhang, B. Chen, S. Wu, M. He and B. Hu, *Talanta*, 2016, **154**, 474–480.
22 L. Nyaba, J. M. Matong, K. M. Dimpe and P. N. Nomngongo, *Talanta*, 2016, **159**, 174–180.
23 P. Niedzielski, *Anal. Chim. Acta*, 2005, **551**, 199–206.
24 J. Fu, X. Zhang, S. Qian and L. Zhang, *Talanta*, 2012, **94**, 167–171.
25 S.-H. Hong, F. N. Lyonga, J.-K. Kang, E.-J. Seo, C.-G. Lee,

S. Jeong, S.-G. Hong and S.-J. Park, *Chemosphere*, 2020, **252**, 126475.
26 M. G. Bordash, E. Pagliano, K. L. LeBlanc, P. Kumkrong, D. Wallschläger and Z. Mester, *Sci. Total Environ.*, 2020, **745**, 140877.
27 C. Shi, G. S. Ding, A. N. Tang and Y. Y. Qiao, *Anal. Methods*, 2017, **9**, 1658–1664.
28 Z. Azizi and A. Babakhanian, *Anal. Methods*, 2018, **10**, 5205–5213.
29 T. A. Ivandini and Y. Einaga, *Electrocatalysis*, 2013, **4**, 367–374.
30 V. Beni, G. Collins and D. W. M. Arrigan, *Anal. Chim. Acta*, 2011, **699**, 127–133.
31 R. W. Andrews and D. C. Johnson, *Anal. Chem.*, 1975, **47**, 294–299.
32 A. V Kolliopoulos, J. P. Metters and C. E. Banks, *Anal. Methods*, 2013, **5**, 851–856.
33 N. Y. Stozhko, Z. V Shalygina and N. A. Malakhova, *J. Anal. Chem.*, 2004, **59**, 374–380.
34 M. De Feudis, R. D'Amato, D. Businelli and M. Guiducci, *Sci. Total Environ.*, 2019, **659**, 131–139.
35 S. Santos, G. Ungureanu, R. Boaventura and C. Botelho, *Sci. Total Environ.*, 2015, **521**–**522**, 246–260.
36 Q. WANG, J. ZHANG, B. ZHAO, X. XIN, X. DENG and H. ZHANG, *Pedosphere*, 2016, **26**, 120–129.
37 H. M. Ohlendorf, R. W. Lowe, P. R. Kelly and T. E. Harvey, *J. Wildl. Manage.*, 1986, **50**, 64–70.
38 L. M. Walker, E. A. Karnaukh, F. Dewan and M. C. Buzzeo, *Electrochem. commun.*, 2016, **69**, 28–31.
39 P. Devi, R. Jain, A. Thakur, M. Kumar, N. K. Labhsetwar, M. Nayak and P. Kumar, *TrAC Trends Anal. Chem.*, 2017, **95**, 69–85.
40 R. Chawla, T. Filippini, R. Loomba, S. Cilloni, K. S. Dhillon and M. Vinceti, *Sci. Total Environ.*, 2020, **719**, 134541.
41 C. Chang, R. Yin, X. Wang, S. Shao, C. Chen and H. Zhang, *Sci. Total Environ.*, 2019, **669**, 83–90.
42 Z. Tan, W. Wu, N. Yin, M. Jia, X. Chen, Y. Bai, H. Wu, Z. Zhang and P. Li, *J. Food Compos. Anal.*, 2020, **94**, 103628.
43 J. Zhu, N. Wang, S. Li, L. Li, H. Su and C. Liu, *Sci. Total Environ.*, 2008, **392**, 252–261.
44 M. J. Melgar, R. Núñez and M. Á. García, *Sci. Total Environ.*, 2019, **694**, 133716.
45 S. O. Okonji, J. A. Dominic, D. Pernitsky and G. Achari, *J. Water Process Eng.*, 2020, **38**, 101666.
46 M. De Feudis, R. D'Amato, D. Businelli and M. Guiducci, *Sci. Total Environ.*, 2019, **659**, 131–139.
47 L. Zhong, Y. Cao, W. Li, K. Xie and W.-P. Pan, *J. Environ. Sci.*, 2011, **23**, 171–176.
48 S. Wu, J. Sun, H. Zhang and H. Mo, *J. Biotechnol.*, 2008, **136**, S724.
49 R. Jagtap and W. Maher, *Microchem. J.*, 2016, **124**, 422–529.
50 E. Vassileva, A. Becker and J. A. C. Broekaert, *Anal. Chim. Acta*, 2001, **441**, 135–146.
51 Y. Zhao, J. Zheng, M. Yang, G. Yang, Y. Wu and F. Fu, *Talanta*, 2011, **84**, 983–988.
52 V. S. Saji and C.-W. Lee, *RSC Adv.*, 2013, **3**, 10058–10077.
53 F. A. Bertolino, A. A. J. Torriero, E. Salinas, R. Olsina, L. D. Martinez and J. Raba, *Anal. Chim. Acta*, 2006, **572**, 32–38.
54 A. O. Idris, N. Mabuba and O. A. Arotiba, *J. Electroanal. Chem.*, 2015, **758**, 7–11.
55 K. L. LeBlanc, P. Kumkrong, P. H. J. Mercier and Z. Mester, *Sci. Total Environ.*, 2018, **640**–**641**, 1635–1651.
56 T. Rasheed, A. A. Hassan, M. Bilal, T. Hussain and K. Rizwan, *Chemosphere*, 2020, **259**, 127369.
57 W. Zhang, *J. Nanoparticle Res.*, 2003, **5**, 323–332.
58 K. Pyrzynska, *Talanta*, 2020, **212**, 120784.
59 P. Zuman and G. Somer, *Talanta*, 2000, **51**, 645–665.
60 P. Sharifian and A. Aliakbar, *Anal. Methods*, 2015, **7**, 2121–2128.
61 M. Zelić and M. Branica, *Electroanalysis*, 1990, **2**, 455–462.
62 I. E. Merino, E. Stegmann, M. E. Aliaga, M. Gomez, V. Arancibia and C. Rojas−Romo, *Anal. Chim. Acta*, 2019, **1048**, 22–30.
63 R. Kowalik, *Arch. Metall. Mater.*
64 T. Ishiyama and T. Tanaka, *Anal. Chem.*, 1996, **68**, 3789–3792.
65 M. Cavallini, G. Aloisi and R. Guidelli, *Langmuir*, 1999, **15**, 2993–2995.
66 B. Baś, K. Jedlińska and K. Węgiel, *Electrochem. commun.*, 2014, **49**, 79–82.
67 L.-H. Wang and X.-E. Shan, *J. Anal. Chem.*, 2016, **71**, 917–925.
68 G. A. Ragoisha, Y. M. Aniskevich, A. S. Bakavets and E. A. Streltsov, *J. Solid State Electrochem.*, 2020, **24**, 2585–2594.
69 B. M. Huang, T. E. Lister and J. L. Stickney, *Surf. Sci.*, 1997, **392**, 27–43.
70 T. E. Lister and J. L. Stickney, *J. Phys. Chem.*, 1996, **100**, 19568–19576.
71 M. Alanyalioglu, U. Demir and C. Shannon, *J. Electroanal. Chem.*, 2004, **561**, 21–27.
72 C. Wei, N. Myung and K. Rajeshwar, *J. Electroanal. Chem.*, 1994, **375**, 109–115.
73 M. C. Santos and S. A. S. Machado, *J. Electroanal. Chem.*, 2004, **567**, 203–210.
74 S. G. Hazelton and D. T. Pierce, *Anal. Chem.*, 2007, **79**, 4558–4563.
75 R. Jain, A. Thakur, P. Kumar and D. Pooja, *Electrochim. Acta*, 2018, **290**, 291–302.
76 S. Iqbal, L. Zan, E. Nardi and H. Baltruschat, *Phys. Chem. Chem. Phys.*, 2018, **20**, 6176–6186.
77 Y. Lai, F. Liu, J. Li, Z. Zhang and Y. Liu, *J. Electroanal. Chem.*, 2010, **639**, 187–192.
78 G. Jarzabek and Z. Kublik, *J. Electroanal. Chem. Interfacial Electrochem.*, 1980, **114**, 165–177.
79 A. M. Espinosa, M. L. Tascón, M. D. Vázquez and P. S. Batanero, *Electrochim. Acta*, 1992, **37**, 1165–1172.
80 A. O. Idris, N. Mabuba, D. Nkosi, N. Maxakato and O. A. Arotiba, *Int. J. Environ. Anal. Chem.*, 2017, **97**, 534–547.

81 M.-S. Won, J.-H. Yoon and Y.-B. Shim, *Electroanalysis*, 2005, **17**, 1952–1958.
82 P. Sharifian and A. Aliakbar, *Anal. Methods*, 2015, **7**, 4321–4327.
83 M. Ashournia and A. Aliakbar, *J. Hazard. Mater.*, 2010, **174**, 788–794.
84 Ş. Kartal, T. Oymak and Ş. Tokalıoğlu, *J. Anal. Chem.*, 2010, **65**, 1221–1227.
85 A. A. Ramadan, H. Mandil and A. Shikh-Debes, *Int J Pharm Pharm Sci*, 2014, **6**, 148–153.
86 A. A. Ramadan, H. Mandil and A. Shikh-Debes, *Res. J. Pharm. Technol.*, 2018, **11**, 2030–2035.
87 A. A. Ramadan, H. Mandil and A. Ozoun, *Asian J. Chem.*, 2013, **25**, 3393.
88 N. Y. Stozhko, E. I. Morosanova, L. I. Kolyadina and S. V Fomina, *J. Anal. Chem.*, 2006, **61**, 158–165.
89 Y. V. Matveichuk, *Vopr. Khimii i Khimicheskoi Tekhnologii*, 2019, **2019**, 80–88.
90 D. W. Bryce, A. Izquierdo and M. D. L. De Castro, *Anal. Chim. Acta*, 1995, **308**, 96–101.
91 C. Dhand, N. Dwivedi, X. J. Loh, A. N. Jie Ying, N. K. Verma, R. W. Beuerman, R. Lakshminarayanan and S. Ramakrishna, *RSC Adv.*, 2015, **5**, 105003–105037.
92 G. A. Cutter, *Anal. Chim. Acta*, 1978, **98**, 59–66.
93 L. A. Escudero, P. H. Pacheco, J. A. Gasquez and J. A. Salonia, *Food Chem.*, 2015, **169**, 73–79.
94 M. Nozohour Yazdi and Y. Yamini, *New J. Chem.*, 2017, **41**, 2378–2385.
95 E. Bağda and M. Tüzen, *Food Chem.*, 2017, **232**, 98–104.
96 D. R. Mees, W. Pysto and P. J. Tarcha, *J. Colloid Interface Sci.*, 1995, **170**, 254–260.
97 G. Zhang, M. A. Gomez, S. Yao, X. Ma, S. Li, X. Cao, S. Zang and Y. Jia, *Environ. Sci. Pollut. Res.*, 2019, **26**, 10159–10173.
98 M. Kazemi, A. Akbari, S. Soleimanpour, N. Feizi and M. Darroudi, *J. Clust. Sci.*, 2019, **30**, 767–775.
99 F. Gao, Q. Lu, X. Meng and S. Komarneni, *J. Mater. Sci.*, 2008, **43**, 2377–2386.
100 B. Zhang, X. Ye, W. Dai, W. Hou, F. Zuo and Y. Xie, *Nanotechnology*, 2005, **17**, 385–390.
101 Z. Chen, Y. Shen, A. Xie, J. Zhu, Z. Wu and F. Huang, *Cryst. Growth Des.*, 2009, **9**, 1327–1333.
102 K. S. Prasad and K. Selvaraj, *Biol. Trace Elem. Res.*, 2014, **157**, 275–283.
103 K. S. Prasad, H. Patel, T. Patel, K. Patel and K. Selvaraj, *Colloids Surfaces B Biointerfaces*, 2013, **103**, 261–266.
104 G. K. Kumar, P. S. Sharma, S. Sounderajan, D. Datta, R. K. Singhal and A. C. Udas, *Anal. Methods*, 2015, **7**, 8262–8270.
105 S. Ramya, T. Shanmugasundaram and R. Balagurunathan, *J. Trace Elem. Med. Biol.*, 2015, **32**, 30–39.
106 B. Li, N. Liu, Y. Li, W. Jing, J. Fan, D. Li, L. Zhang, X. Zhang, Z. Zhang and L. Wang, *PLoS One*, 2014, **9**, e95955.
107 N. Patel, A. Kaler, S. Jain and U. Chand Banerjee, *Curr. Nanosci.*, 9, 463–468.
108 H. Kimura, T.-H. Arima, T. Oku and T. Sakaguchi, *Asia Pacific J. Sustain. Agric. Food Energy*, 2014, **2**, 5–8.
109 S. P. W. Hageman, R. D. van der Weijden, J. Weijma and C. J. N. Buisman, *Water Res.*, 2013, **47**, 2118–2128.
110 A. Abdelouas, W. L. Gong, W. Lutze, J. A. Shelnutt, R. Franco and I. Moura, *Chem. Mater.*, 2000, **12**, 1510–1512.
111 S. M. Etezad, K. Khajeh, M. Soudi, P. T. M. Ghazvini and B. Dabirmanesh, *Enzyme Microb. Technol.*, 2009, **45**, 1–6.
112 C. A. Watts, H. Ridley, K. L. Condie, J. T. Leaver, D. J. Richardson and C. S. Butler, *FEMS Microbiol. Lett.*, 2003, **228**, 273–279.
113 H. K. Hansen, S. F. Peña, C. Gutiérrez, A. Lazo, P. Lazo and L. M. Ottosen, *J. Hazard. Mater.*, 2019, **364**, 78–81.
114 V. K. Kovatcheva and M. D. Parlapanski, *Colloids Surfaces A Physicochem. Eng. Asp.*, 1999, **149**, 603–608.
115 H. K. Hansen, S. Franco Peña, C. Gutiérrez and P. Núñez, *Water Environ. J.*, 2020, **34**, 284–290.
116 Y. Wu, C.-Y. Guan, N. Griswold, L. Hou, X. Fang, A. Hu, Z. Hu and C.-P. Yu, *J. Clean. Prod.*, 2020, **277**, 123478.
117 F. Fu, D. D. Dionysiou and H. Liu, *J. Hazard. Mater.*, 2014, **267**, 194–205.
118 H. Qin, J. Li, H. Yang, B. Pan, W. Zhang and X. Guan, *Environ. Sci. Technol.*, 2017, **51**, 5090–5097.
119 C. Tang, Y. H. Huang, H. Zeng and Z. Zhang, *Chem. Eng. J.*, 2014, **244**, 97–104.
120 F. Fu, J. Lu, Z. Cheng and B. Tang, *Ultrason. Sonochem.*, 2016, **29**, 328–336.
121 L. Liang, W. Sun, X. Guan, Y. Huang, W. Choi, H. Bao, L. Li and Z. Jiang, *Water Res.*, 2014, **49**, 371–380.
122 P. Fan, L. Li, Y. Sun, J. Qiao, C. Xu and X. Guan, *Water Res.*, 2019, **159**, 375–384.
123 H. Dong, Y. Chen, G. Sheng, J. Li, J. Cao, Z. Li and Y. Li, *J. Hazard. Mater.*, 2016, **304**, 306–312.
124 J. Filip, J. Kolařík, E. Petala, M. Petr, O. Šráček and R. Zbořil, eds. T. Phenrat and G. V Lowry, Springer International Publishing, Cham, 2019, pp. 157–199.
125 L. Ling, B. Pan and W. Zhang, *Water Res.*, 2015, **71**, 274–281.
126 J. T. Olegario, N. Yee, M. Miller, J. Sczepaniak and B. Manning, *J. Nanoparticle Res.*, 2010, **12**, 2057–2068.
127 Z. Qi, R. Liu, T. P. Joshi, J. Peng and J. Qu, *Chem. Eng. J.*, 2021, **405**, 126564.
128 K. Mondal, G. Jegadeesan and S. B. Lalvani, *Ind. Eng. Chem. Res.*, 2004, **43**, 4922–4934.
129 G. Sheng, A. Alsaedi, W. Shammakh, S. Monaquel, J. Sheng, X. Wang, H. Li and Y. Huang, *Carbon N. Y.*, 2016, **99**, 123–130.
130 Q. Wang, Y. Zhao, W. Luo, W. Jiang, J. Fan, L. Wang, W. Jiang, W. Zhang and J. Yang, *Chem. Commun.*, 2018, **54**, 5887–5890.
131 C. Shan, X. Wang, X. Guan, F. Liu, W. Zhang and B. Pan, *Ind. Eng. Chem. Res.*, 2017, **56**, 5309–5317.
132 B. Hu, G. Chen, C. Jin, J. Hu, C. Huang, J. Sheng, G. Sheng, J. Ma and Y. Huang, *J. Hazard. Mater.*, 2017, **336**, 214–221.

133 L. S. Balistrieri and T. T. Chao, *Soil Sci. Soc. Am. J.*, 1987, **51**, 1145–1151.

134 M. Martínez, J. Giménez, J. de Pablo, M. Rovira and L. Duro, *Appl. Surf. Sci.*, 2006, **252**, 3767–3773.

135 K. Kalaitzidou, A.-A. Nikoletopoulos, N. Tsiftsakis, F. Pinakidou and M. Mitrakas, *Sci. Total Environ.*, 2019, **687**, 1197–1206.

136 C. Su and D. L. Suarez, *Soil Sci. Soc. Am. J.*, 2000, **64**, 101–111.

137 N. Zhang, D. D. Gang, L. McDonald and L.-S. Lin, *Chemosphere*, 2018, **195**, 166–174.

138 M. Matulová, M. Bujdoš, M. B. Miglierini, Z. Mitróová, M. Kubovčíková and M. Urík, *Chem. Geol.*, 2020, **556**, 119852.

139 M. O. M. Sharrad, H. Liu and M. Fan, *Sep. Purif. Technol.*, 2012, **84**, 29–34.

140 C. M. Gonzalez, J. Hernandez, J. R. Peralta-Videa, C. E. Botez, J. G. Parsons and J. L. Gardea-Torresdey, *J. Hazard. Mater.*, 2012, **211**–**212**, 138–145.

141 M. Rovira, J. Giménez, M. Martínez, X. Martínez-Lladó, J. de Pablo, V. Martí and L. Duro, *J. Hazard. Mater.*, 2008, **150**, 279–284.

142 Z. Ning, G. Dianchen and L. Lian-Shin, *J. Environ. Eng.*, 2010, **136**, 1089–1095.

143 A. S. Jadhav, M. Ali Amrani, S. K. Singh, A. S. Al-Fatesh, A. Bansiwal, V. V. S. S. Srikanth and N. K. Labhasetwar, *J. Water Process Eng.*, 2020, **37**, 101396.

144 O. Y. Bakather, A. Kayvani Fard, Ihsanullah, M. Khraisheh, M. S. Nasser and M. A. Atieh, *Bioinorg. Chem. Appl.*, 2017, **2017**, 4323619.

145 Q. T. Dinh, Z. Li, T. A. T. Tran, D. Wang and D. Liang, *Chemosphere*, 2017, **184**, 618–635.

146 D. Fang, S. Wei, Y. Xu, J. Xiong and W. Tan, *Sci. Total Environ.*, 2019, **684**, 694–704.

147 T. P. Rao, M. Anbu, M. L. P. Reddy, C. S. P. Iyer and A. D. Damodaran, *Anal. Lett.*, 1996, **29**, 2563–2571.

148 S. Goldberg, *Soil Sci. Soc. Am. J.*, 2014, **78**, 473–479.

149 C.-H. Wu, S.-L. Lo and C.-F. Lin, *Colloids Surfaces A Physicochem. Eng. Asp.*, 2000, **166**, 251–259.

150 T. Su, X. Guan, G. Gu and J. Wang, *J. Colloid Interface Sci.*, 2008, **326**, 347–353.

151 J. Ayala and B. Fernández, *JOM*, 2015, **67**, 2727–2732.

152 J. S. Yamani, A. W. Lounsbury and J. B. Zimmerman, *Water Res.*, 2014, **50**, 373–381.

153 C. Huang, B. Hu, M. He and J. Duan, *J. Mass Spectrom.*, 2008, **43**, 336–345.

154 E. Tahmasebi, *J. Mol. Liq.*, 2020, **299**, 112111.

155 S. A. Davis and M. Misra, *J. Colloid Interface Sci.*, 1997, **188**, 340–350.

156 W. Cui, P. Li, Z. Wang, S. Zheng and Y. Zhang, *J. Hazard. Mater.*, 2018, **341**, 268–276.

157 J. Devoy, A. Walcarius and J. Bessiere, *Langmuir*, 2002, **18**, 8472–8480.

158 A. Walcarius, J. Devoy and J. Bessière, *Langmuir*, 2004, **20**, 6335–6343.

159 B. A. Labaran and M. S. Vohra, *Desalin. Water Treat.*, 2018, **124**, 267–278.

160 S. Li and N. Deng, *Anal. Bioanal. Chem.*, 2002, **374**, 1341–1345.

161 L. Svecova, M. Dossot, S. Cremel, M.-O. Simonnot, M. Sardin, B. Humbert, C. Den Auwer and L. J. Michot, *J. Hazard. Mater.*, 2011, **189**, 764–772.

162 G. Sheng, W. Linghu, Z. Chen, D. Xu, A. Alsaedi, W. Shammakh, S. Monaquel and J. Sheng, *Environ. Nanotechnology, Monit. Manag.*, 2016, **6**, 152–158.

163 B. Zawisza, R. Sitko, I. Queralt, E. Margui and A. Gagor, *Microchim. Acta*, 2020, **187**, 430.

164 T. Yu, B. Liu and J. Liu, *J. Anal. Test.*, 2017, **1**, 2.

165 W. Sun, W. Pan, F. Wang and N. Xu, *Chem. Eng. J.*, 2015, **273**, 353–362.

166 Y. T. Chan, W. H. Kuan, T. Y. Chen and M. K. Wang, *Water Res.*, 2009, **43**, 4412–4420.

167 M. Thakkar and S. Mitra, *J. Nanomater.*, 2017, **2017**, 1734643.

168 X. Wu, X. Guo and L. Zhang, *Ind. Eng. Chem. Res.*, 2019, **58**, 342–349.

169 G. M. Rashad, M. A. Soliman and M. R. Mahmoud, *J. Radioanal. Nucl. Chem.*, 2018, **317**, 593–603.

170 T. M. Suzuki, M. L. Tanco, D. A. Pacheco Tanaka, H. Matsunaga and T. Yokoyama, *Sep. Sci. Technol.*, 2001, **36**, 103–111.

171 P. Gurunathan, S. Hari, S. B. Suseela, R. Sankararajan and A. Mukannan, *Environ. Sci. Pollut. Res.*, 2019, **26**, 528–543.

172 T. Suzuki, K. Sue, H. Morotomi, M. Niinae, M. Yokoshima and H. Nakata, *J. Environ. Chem. Eng.*, 2019, **7**, 102802.

173 Q. Tian, B. Guo, C. Chuaicham and K. Sasaki, *Chemosphere*, 2020, **248**, 126123.

174 K.-H. Goh, T.-T. Lim and Z. Dong, *Water Res.*, 2008, **42**, 1343–1368.

175 G. A. O'neill, C. Misra and A. S. C. Chen, 1991.

176 N. Chubar and M. Szlachta, *Chem. Eng. J.*, 2015, **279**, 885–896.

177 K.-H. Goh, T.-T. Lim, A. Banas and Z. Dong, *J. Hazard. Mater.*, 2010, **179**, 818–827.

178 M. Li, A. Dopilka, A. N. Kraetz, H. Jing and C. K. Chan, *Ind. Eng. Chem. Res.*, 2018, **57**, 4978–4987.

179 M.-L. Chen and M.-I. An, *Talanta*, 2012, **95**, 31–35.

180 S. XU, D. LI, X. GUO, W. YAN and J. GAO, *Trans. Nonferrous Met. Soc. China*, 2019, **29**, 1763–1775.

181 D. Li, W. Yan, X. Guo, Q. Tian, Z. Xu and L. Zhu, *Hydrometallurgy*, 2020, **191**, 105231.

182 M. Li, L. M. Farmen and C. K. Chan, *Ind. Eng. Chem. Res.*, 2017, **56**, 2458–2465.

183 Y. Wu, Y. Chi, H. Bai, G. Qian, Y. Cao, J. Zhou, Y. Xu, Q. Liu, Z. P. Xu and S. Qiao, *J. Hazard. Mater.*, 2010, **176**, 193–198.

184 F. Geng, H. Xin, Y. Matsushita, R. Ma, M. Tanaka, F. Izumi, N. Iyi and T. Sasaki, *Chem. – A Eur. J.*, 2008, **14**, 9255–9260.

185 L. Zhu, L. Zhang, J. Li, D. Zhang, L. Chen, D. Sheng, S. Yang, C. Xiao, J. Wang, Z. Chai, T. E. Albrecht-Schmitt and S. Wang, *Environ. Sci. Technol.*, 2017, **51**, 8606–

8615.
186 Q. Tian and K. Sasaki, *Sci. Total Environ.*, 2019, **695**, 133799.
187 P. Koilraj, Y. Kamura and K. Sasaki, *ACS Sustain. Chem. Eng.*, 2018, **6**, 13854–13866.
188 P. Koilraj, Y. Kamura and K. Sasaki, *J. Mater. Chem. A*, 2018, **6**, 10008–10018.
189 L. Xu and Y. Huang, *Chem. Eng. J.*, 2019, **359**, 1166–1174.
190 M. Kang, F. Chen, S. Wu, Y. Yang, C. Bruggeman and L. Charlet, *Environ. Sci. Technol.*, 2011, **45**, 2704–2710.
191 A. Naveau, F. Monteil-Rivera, E. Guillon and J. Dumonceau, *Environ. Sci. Technol.*, 2007, **41**, 5376–5382.
192 C. Bruggeman, A. Maes, J. Vancluysen and P. Vandemussele, *Environ. Pollut.*, 2005, **137**, 209–221.
193 P. Cook, Y. Kim, K. Yuan, M. C. Marcano and U. Becker, *Minerals*, 2019, **9**, 437.
194 M. Duc, G. Lefevre, M. Fedoroff, J. Jeanjean, J. C. Rouchaud, F. Monteil-Rivera, J. Dumonceau and S. Milonjic, *J. Environ. Radioact.*, 2003, **70**, 61–72.
195 S. Kongsri, K. Janpradit, K. Buapa, S. Techawongstien and S. Chanthai, *Chem. Eng. J.*, 2013, **215–216**, 522–532.
196 F. Monteil-Rivera, M. Fedoroff, J. Jeanjean, L. Minel, M.-G. Barthes and J. Dumonceau, *J. Colloid Interface Sci.*, 2000, **221**, 291–300.
197 H. He, J. Liu, Y. Dong, H. Li, S. Zhao, J. Wang, M. Jia, H. Zhang, J. Liao, J. Yang, Y. Yang and N. Liu, *J. Environ. Radioact.*, 2019, **203**, 210–219.
198 M. Krawczyk-Coda, *Food Anal. Methods*, 2019, **12**, 128–135.
199 X. Zhang, X. Li, F. Zhang, S. Peng, S. H. Tumrani and X. Ji, *J. Water Reuse Desalin.*, 2019, **9**, 506–519.
200 J. He, X. Qiao, Y. Shi, Y. Li, X. Yang, W. Zhou and C. Liu, *Sci. China Chem.*, 2017, **60**, 1258–1264.
201 G. M. Haggerty and R. S. Bowman, *Environ. Sci. Technol.*, 1994, **28**, 452–458.
202 J. Behnsen and B. Riebe, *Appl. Geochemistry*, 2008, **23**, 2746–2752.
203 U. K. Saha, C. Liu, L. M. Kozak and P. M. Huang, *Soil Sci. Soc. Am. J.*, 2004, **68**, 1197–1209.
204 E. Orucoglu and S. Haciyakupoglu, *J. Environ. Manage.*, 2015, **160**, 30–38.
205 S. Haciyakupoglu and E. Orucoglu, *Appl. Clay Sci.*, 2013, **86**, 190–198.
206 H. Wang, T. Wu, J. Chen, Q. Zheng, C. He and Y. Zhao, *J. Radioanal. Nucl. Chem.*, 2015, **303**, 107–113.
207 J. Phanthasri, N. Grisdanurak, P. Khamdahsag, K. Wantala, R. Khunphonoi, S. Wannapaiboon and V. Tanboonchuy, *Water, Air, Soil Pollut.*, 2020, **231**, 199.
208 Q. Tian, B. Guo and K. Sasaki, *J. Hazard. Mater.*, 2020, **387**, 121994.
209 S. M. Shaheen, N. K. Niazi, N. E. E. Hassan, I. Bibi, H. Wang, D. C. W. Tsang, Y. S. Ok, N. Bolan and J. Rinklebe, *Int. Mater. Rev.*, 2019, **64**, 216–247.
210 S. Peräniemi, S. Hannonen, H. Mustalahti and M. Ahlgrén, *Fresenius. J. Anal. Chem.*, 1994, **349**, 510–515.
211 S. Latva, S. Peräniemi and M. Ahlgrén, *Anal. Chim. Acta*, 2003, **478**, 229–235.
212 X. Zhao, A. Zhang, J. Zhang, Q. Wang, X. Huang, Y. Wu and C. Tang, *Materials (Basel).*, 2020, **13**, 468.
213 N. Zhang and D. Gang, in *Proceedings of the IASTED International Conference*, vol. 650, p. 60.
214 D. A. Roberts, N. A. Paul, S. A. Dworjanyn, Y. Hu, M. I. Bird and R. de Nys, *J. Appl. Phycol.*, 2015, **27**, 611–620.
215 P. Godlewska, A. Bogusz, J. Dobrzyńska, R. Dobrowolski and P. Oleszczuk, *J. Saudi Chem. Soc.*, 2020, **24**, 824–834.
216 R. Dobrowolski and M. Otto, *Chemosphere*, 2013, **90**, 683–690.
217 C. L. Johansson, N. A. Paul, R. de Nys and D. A. Roberts, *J. Environ. Manage.*, 2016, **165**, 117–123.
218 C. L. Johansson, N. A. Paul, R. de Nys and D. A. Roberts, *J. Environ. Manage.*, 2015, **151**, 386–392.
219 E. I. El-Shafey, *J. Hazard. Mater.*, 2007, **147**, 546–555.
220 H. Khakpour, H. Younesi and M. Mohammadhosseini, *J. Environ. Chem. Eng.*, 2014, **2**, 532–542.
221 S. Dev, A. Khamkhash, T. Ghosh and S. Aggarwal, *ACS Omega*, 2020, **5**, 17215–17222.
222 H. Niu and B. Volesky, *Hydrometallurgy*, 2003, **71**, 209–215.
223 D. M. G. Saad, E. M. Cukrowska and H. Tutu, *Toxicol. Environ. Chem.*, 2013, **95**, 409–421.
224 T. Nishimura, H. Hashimoto and M. Nakayama, *Sep. Sci. Technol.*, 2007, **42**, 3155–3167.
225 Y. Mo, T. Vincent, C. Faur and E. Guibal, *Int. J. Biol. Macromol.*, 2020, **147**, 832–843.
226 X. Min, D. Trujillo, J. Huo, Q. Dong and Y. Wang, *Chem. Eng. J.*, 2020, **396**, 125278.
227 S. Fındık, M. Gülfen and A. O. Aydın, *Sep. Sci. Technol.*, 2014, **49**, 2890–2896.
228 C. Gerente, V. K. C. Lee, P. Le Cloirec and G. McKay, *Crit. Rev. Environ. Sci. Technol.*, 2007, **37**, 41–127.
229 S. Déon, J. Deher, B. Lam, N. Crini, G. Crini and P. Fievet, *Ind. Eng. Chem. Res.*, 2017, **56**, 10461–10471.
230 M. Li, A. Dopilka, A. N. Kraetz, H. Jing and C. K. Chan, *Ind. Eng. Chem. Res.*, 2018, **57**, 4978–4987.
231 T. L. Chua, C. E. Mejia, R. E. R., N. Y. V., van H. E. D. and L. P. N. L., *J. Environ. Eng.*, 2018, **144**, 4018110.
232 Y. He, Y. P. Tang and T. S. Chung, *Ind. Eng. Chem. Res.*, 2016, **55**, 12929–12938.
233 A. Guleria, S. Neogy, B. S. Raorane and S. Adhikari, *Mater. Chem. Phys.*, 2020, **253**, 123369.
234 I. A. Dereven'kov, P. A. Molodtsov and S. V Makarov, *React. Kinet. Mech. Catal.*, 2020, **131**, 555–566.
235 M. Min, C. Shen, L. Fang, B. Zhu, J. Li, L. Yao, Y. Jiang and C. Xiong, *Chem. Eng. Res. Des.*, 2017, **117**, 773–783.
236 M.-Q. Yu, G.-Q. Liu and Q. Jin, *Talanta*, 1983, **30**, 265–270.
237 M. Min, C. Shen, L. Fang, Y. Chang, J. Li, Y. Jiang and C. Xiong, *Anal. Methods*, 2016, **8**, 8084–8091.
238 A.-L. Pommier, S. Simon, R. Buzier and G. Guibaud, *Talanta*, 2019, **199**, 590–595.

239 P. H. Pacheco, R. A. Gil, P. Smichowski, G. Polla and L. D. Martinez, *J. Anal. At. Spectrom.*, 2007, **22**, 305–309.

240 M. Llaver and R. G. Wuilloud, *Microchem. J.*, 2019, **146**, 763–770.

241 K. Kocot, R. Leardi, B. Walczak and R. Sitko, *Talanta*, 2015, **134**, 360–365.

242 N. Gezer, M. Gülfen and A. O. Aydın, *J. Appl. Polym. Sci.*, 2011, **122**, 1134–1141.

243 L. Yan, B. Deng, C. Shen, C. Long, Q. Deng and C. Tao, *J. Chromatogr. A*, 2015, **1395**, 173–179.

244 F. Sahin, M. Volkan, A. G. Howard and O. Y. Ataman, *Talanta*, 2003, **60**, 1003–1009.

245 W. Warkocki, S. A. El-Safty, M. A. Shenashen, E. Elshehy, H. Yamaguchi and N. Akhtar, *J. Mater. Chem. A*, 2015, **3**, 17578–17589.

246 A. N. Acikkapi, M. Tuzen and B. Hazer, *Food Chem.*, 2019, **284**, 1–7.

247 D. Santra and K. Sen, *Int. J. Biol. Macromol.*, 2019, **122**, 395–404.

248 Y. He, J. Liu, G. Han and T.-S. Chung, *J. Memb. Sci.*, 2018, **555**, 299–306.

249 Z. D. Firouzabadi, S. Dadfarnia, A. M. Haji Shabani, M. H. Ehrampoush and E. N. Tafti, *Int. J. Environ. Anal. Chem.*, 2018, **98**, 555–569.

250 S. Barua, I. M. M. Rahman, M. Miyaguchi, K. Yunoshita, P. Ruengpirasiri, Y. Takamura, A. S. Mashio and H. Hasegawa, *Microchem. J.*, 2020, **159**, 105490.

251 T. M. Suzuki, D. A. Pacheco Tanaka, M. A. Llosa Tanco, M. Kanesato and T. Yokoyama, *J. Environ. Monit.*, 2000, **2**, 550–555.

252 T. Yokoi, T. Tatsumi and H. Yoshitake, *J. Colloid Interface Sci.*, 2004, **274**, 451–457.

253 H. Yoshitake and R. Otsuka, *Langmuir*, 2013, **29**, 10513–10520.

254 J. S. Yamani, A. W. Lounsbury and J. B. Zimmerman, *Water Res.*, 2016, **88**, 889–896.

255 M. S. Seyed Dorraji, A. R. Amani-Ghadim, Y. Hanifehpour, S. Woo Joo, A. Figoli, M. Carraro and F. Tasselli, *Chem. Eng. Res. Des.*, 2017, **117**, 309–317.

256 H. Takada, Y. Watanabe and M. Iwamoto, *Chem. Lett.*, 2003, **33**, 62–63.

257 A. J. Howarth, M. J. Katz, T. C. Wang, A. E. Platero-Prats, K. W. Chapman, J. T. Hupp and O. K. Farha, *J. Am. Chem. Soc.*, 2015, **137**, 7488–7494.

258 R. J. Drout, A. J. Howarth, K. Otake, T. Islamoglu and O. K. Farha, *CrystEngComm*, 2018, **20**, 6140–6145.

259 J. Wei, W. Zhang, W. Pan, C. Li and W. Sun, *Environ. Sci. Nano*, 2018, **5**, 1441–1453.

260 S. Sharma, A. V Desai, B. Joarder and S. K. Ghosh, *Angew. Chemie Int. Ed.*, 2020, **59**, 7788–7792.

261 J. Li, Y. Liu, X. Wang, G. Zhao, Y. Ai, B. Han, T. Wen, T. Hayat, A. Alsaedi and X. Wang, *Chem. Eng. J.*, 2017, **330**, 1012–1021.

262 H. Ouyang, N. Chen, G. Chang, X. Zhao, Y. Sun, S. Chen, H. Zhang and D. Yang, *Angew. Chemie Int. Ed.*, 2018, **57**, 13197–13201.

263 H. Kalantari and M. Manoochehri, *Microchim. Acta*, 2018, **185**, 196.

264 M. Khajeh, Y. Yamini, E. Ghasemi, J. Fasihi and M. Shamsipur, *Anal. Chim. Acta*, 2007, **581**, 208–213.

265 G. C. de Lima, A. C. do Lago, A. A. Chaves, P. S. Fadini and P. O. Luccas, *Anal. Chim. Acta*, 2013, **768**, 35–40.

266 R. Hu, X. Zhang, K.-N. Chi, T. Yang and Y.-H. Yang, *ACS Appl. Mater. Interfaces*, 2020, **12**, 30770–30778.

267 J. A. Cruz-Navarro, F. Hernandez-Garcia and G. A. Alvarez Romero, *Coord. Chem. Rev.*, 2020, **412**, 213263.

268 M. Lu, Y. Deng, Y. Luo, J. Lv, T. Li, J. Xu, S.-W. Chen and J. Wang, *Anal. Chem.*, 2019, **91**, 888–895.

269 M. A. Djebbi, S. Boubakri, M. Braiek, N. Jaffrezic-Renault, P. Namour and A. B. H. Amara, *Electroanalysis*, 2020, **32**, 1186–1197.

270 C. A. Sanchez, J. A. Rodríguez, M. E. Paez-Hernandez, E. M. Santos and Y. Castrillejo, *Electroanalysis*, 2019, **31**, 329–334.

271 L. Rassaei, F. Marken, M. Sillanpää, M. Amiri, C. M. Cirtiu and M. Sillanpää, *TrAC Trends Anal. Chem.*, 2011, **30**, 1704–1715.

272 Q. Chen, R. Ding, H. Liu, L. Zhou, Y. Wang, Y. Zhang and G. Fan, *ACS Appl. Mater. Interfaces*, 2020, **12**, 12919–12929.

273 Z. Zhao, Y. Sun, J. Song, Y. Li, Y. Xie, H. Cui, W. Gong, J. Hu and Y. Chen, *Sensors Actuators B Chem.*, 2021, **326**, 128811.

274 X. Xia, L. Ling and W. Zhang, *Environ. Sci. Nano*, 2017, **4**, 52–59.